Title

Farmed fur animals harbour viruses with zoonotic spillover potential.

Journal

Nature: New biology, 634(8032)

Authors

Zhao, Jin
Wan, Wenbo
Yu, Kang
et al.

Publication Date

2024-10-01

DOI

10.1038/s41586-024-07901-3

Peer reviewed

HHS Public Access

Author manuscript

Nature. Author manuscript; available in PMC 2025 January 17.

Published in final edited form as:

Nature. 2024 October ; 634(8032): 228–233. doi:10.1038/s41586-024-07901-3.

Farmed fur animals harbour viruses with zoonotic spillover potential

Jin Zhao[1,13], **Wenbo Wan**[1,13], **Kang Yu**[1,2,13], **Philippe Lemey**[3,13], **John H.-O. Pettersson**[4,5,6,13], **Yuhai Bi**[7,13,14], **Meng Lu**[1], **Xinxin Li**[8], **Zhuohang Chen**[1], **Mengdi Zheng**[8], **Ge Yan**[2], **JianJun Dai**[2], **Yuxing Li**[1], **Ayidana Haerheng**[1], **Na He**[1], **Changchun Tu**[9], **Marc A. Suchard**[10], **Edward C. Holmes**[11,12,13,14], **Wan-Ting He**[2,14,*], **Shuo Su**[1,14,*]

[1]Department of Epidemiology, School of Public Health, Shanghai Institute of Infectious Disease and Biosecurity, Fudan University, Shanghai 200032, China.

[2]State Key Laboratory of Natural Medicines, School of Pharmacy, China Pharmaceutical University, Nanjing 211198, China.

[3]Department of Microbiology, Immunology and Transplantation, Rega Institute, Laboratory for Clinical and Epidemiological Virology, KU Leuven, Leuven 3000, Belgium.

[4]Clinical Microbiology, Department of Medical Sciences, University of Uppsala, SE-751 23 Uppsala, Sweden.

[5]Clinical Microbiology and Hospital Hygiene, Uppsala University Hospital, SE-752 37 Uppsala, Sweden.

[6]Department of Microbiology and Immunology, Peter Doherty Institute for Infection and Immunity, University of Melbourne, Melbourne, VIC, Australia

[7]CAS Key Laboratory of Pathogen Microbiology and Immunology, Institute of Microbiology, Chinese Academy of Sciences (CAS), Beijing 100101, China.

[8]Jiangsu Engineering Laboratory of Animal Immunology, Institute of Immunology, College of Veterinary Medicine, Academy for Advanced Interdisciplinary Studies, Nanjing Agricultural University, Nanjing 210095, China.

[9]Changchun Veterinary Research Institute, Chinese Academy of Agricultural Sciences, Changchun 130122, China

[*]Correspondence: Shuo Su (shuosu@fudan.edu.cn) or (ssh5658485@163.com) and Wan-Ting He (hewt@cpu.edu.cn).

[13]These authors contributed equally: Jin Zhao, Wenbo Wan, Kang Yu, Philippe Lemey, John H.-O. Pettersson, Yuhai Bi, Edward C. Holmes.

[14]These authors jointly supervised this work: Yuhai Bi, Edward C. Holmes, Wan-Ting He, Shuo Su.

Author contributions

S.S., and W.T.H. designed and supervised the research. Y.B., J.Z., X.L., and M.Z. collected samples. J.Z., X.L., M.Z., and G.Y. performed the Sanger sequencing and molecular detection. J.Z., W.W., K.Y., M.L., and W.T.H. performed the genome assembly, annotation and analysis of abundance. J.Z., P.L., W.T.H. and S.S performed the genomic and evolutionary analysis and interpretation. J.H.O.P., Z.C., Y.L., C.T., A.H., N.H., and M.A.S. assisted in the data interpretation. S.S., W.T.H., J.Z., J.H.O.P., E.H., Y.B., W.W., K.Y., and M.L. wrote the paper. All authors reviewed and edited the paper.

Competing interests

The authors declare no competing interests.

[10]Department of Biostatistics, Fielding School of Public Health, and Departments of Biomathematics and Human Genetics, David Geffen School of Medicine, University of California, Los Angeles, Los Angeles, CA 90095, USA.

[11]School of Medical Sciences, The University of Sydney, Sydney, NSW 2006, Australia.

[12]Laboratory of Data Discovery for Health Limited, Hong Kong SAR, China.

Abstract

Animals such as raccoon dogs, mink and muskrats are farmed for fur and are sometimes used as food or medicinal products[1,2], yet they are also potential reservoirs of emerging pathogens[3]. Here we performed single-sample metatranscriptomic sequencing of internal tissues from 461 individual fur animals that were found dead due to disease. We characterized 125 virus species, including 36 that were novel and 39 at potentially high risk of cross-species transmission, including zoonotic spillover. Notably, we identified seven species of coronaviruses, expanding their known host range, and documented the cross-species transmission of a novel canine respiratory coronavirus to raccoon dogs and of bat HKU5-like coronaviruses to mink, present at a high abundance in lung tissues. Three subtypes of influenza A virus – H1N2, H5N6 and H6N2 – were detected in the lungs of guinea pig, mink and muskrat, respectively. Multiple known zoonotic viruses, such as *Japanese encephalitis virus* and *Mammalian orthoreovirus*[4,5], were detected in guinea pigs. Raccoon dogs and mink carried the highest number of potentially high-risk viruses, while viruses from the *Coronaviridae*, *Paramyxoviridae* and *Sedoreoviridae* families commonly infected multiple hosts. These data also reveal potential virus transmission between farmed animals and wild animals, and from humans to farmed animals, indicating that fur farming represents an important transmission hub for viral zoonoses.

Keywords

fur animals; virome; meta-transcriptomics; cross-species transmission; coronavirus; influenza A virus

Introduction

The cross-species transmission of viruses from animals to humans drives infectious disease emergence, occasionally resulting in global pandemics[6–9]. Mammalian wildlife and farmed animals carry a wide diversity of potentially zoonotic viruses[10–14], acting as hubs for the onward transmission of emerging pathogens. However, there has been a lack of surveillance to determine which animal species are most likely to carry zoonotic viruses and which viruses are of greatest risk of emerging in humans[11,13,15,16]. As there is often limited overlap between wildlife and humans, secondary contact with farmed animals may constitute a probable route through which zoonotic viruses are transmitted to humans[17–19]. Virological surveillance of farmed animals therefore provides an opportunity to address these potentially public health issues[10,11].

Current virus-related research on farmed mammals focuses disproportionately on conventional livestock, such as swine. In addition to conventional farmed animals, farmed

fur animals have special economic and modern fashion cultural importance in many countries. Common farmed fur animals include a wide range of species and taxonomic groups, ranging from rodents (such as muskrats, nutria and guinea pigs), carnivores (such as mink and foxes) to even-toed ungulates (such as deer). Many countries farm particular fur animals for national and international fur trade exchanges. Importantly, fur animals such as foxes, civets and mink have been suggested to be the potential hosts for a variety of human viruses, including influenza A virus (IAV), SARS-CoV, and SARS-CoV-2[20–23], and outbreaks of H5N1 IAV have recently been reported in farmed European mink[14]. As humans regularly come into contact with farmed animals, it is critical to improve our knowledge of the viruses that circulate among farmed fur animals and their potential for zoonotic transmission.

Most metagenomic studies of animal viruses generally pool individual animal samples, organized by species or sampling location. Although pooling is an efficient way to examine virus diversity and evolution[24], it hinders the investigation of viral prevalence, co-infection and the detection of low-abundance viruses within individual animals. Moreover, most metagenomic studies of wildlife and farmed special economic animals are based on faecal sampling, such that viruses may have originated from the consumption of other animals or from hosts present in the same environment [25–27]. Fewer studies have considered other tissue types, particularly those sampled from diseased animals. Here we address these issues by sequencing individual organs of animals that probably died as a result of infectious disease.

Asia is one of the most active regions for fur animal farming and trading[28,29]. Despite this, little is known about the viruses that circulate in fur animals in this region. To fill this gap, we sampled farmed and wild fur animals across China, including species that were previously ignored in virological studies. Our analyses provide resources for research into the diversity of viruses that circulate among farmed fur animals, as well as a means to assess whether particular animal species are at heightened risk of carrying potentially zoonotic viruses.

Results

Sampling and sequencing of fur animals for virome analyses

All animal samples were categorized into two groups on the basis of species breeding intensity and distribution in China: (i) the “main” farmed fur animals, and (ii) multipurpose (other) farmed animals. The main farmed fur animals comprised four species (order *Carnivora*) that can be farmed only for fur and not for food consumption: *Neogale vison* (mink), *Vulpes vulpes* (red fox), *Vulpes lagopus* (Arctic fox), and *Nyctereutes procyonoides* (raccoon dog). We sampled 164 individuals from these four species, 116 of which came from four provinces, of which official statistics show that they have intensive breeding programs (Hebei, Shandong, Heilongjiang and Liaoning). The remaining 48 animals were sampled from six other Chinese provinces. For the multipurpose animals bred for food consumption, traditional medicine and fur purposes, we sampled 297 animals comprising 24 species from 5 mammalian orders and covering 25 provinces/municipalities: *Carnivora* (n = 34, 7 species), *Artiodactyla* (n = 34, 7 species), *Rodentia* (n = 157, 6 species),

Diprotodontia (n = 3, 3 species), and *Lagomorpha* (n = 69, 1 species) (Fig. 1a and Supplementary Fig. 1a). Of the total of 461 fur animals sampled, 412 (158 main fur animals, 254 multipurpose animals) originated from breeding environments, and 49 (6 main fur animals, 43 multipurpose animals) came from wild sources (Fig. 1b (left)). Here, "wild" refers to animals that live in natural or artificially created wild environments, such as wildlife sanctuaries.

On the basis of clinical signs predominantly manifested as respiratory and gastrointestinal disease, we collected lung and intestinal tissues for single-tissue library construction. In total, 697 tissue samples were collected, comprising 441 intestine samples, 255 lung samples and 1 liver sample from one wild *Cervus nippon* (sika deer) (Fig. 1b (right)). Most libraries had good sequencing quality (mean quality score of 20 = 95.2%). Among libraries that contained viruses, more than half had more than 3,398 viral reads (Fig. 1c).

Viromes of farmed and wild fur animals

To focus on vertebrate-associated viruses (that is, those that display close phylogenetic relationships to viruses that are known to infect vertebrates), we excluded non-vertebrate-associated viruses from our analysis. Accordingly, we identified and PCR-validated 125 probable vertebrate-associated viruses, encompassing 101 species of RNA virus from 16 families (*Arteriviridae*, *Astroviridae*, *Caliciviridae, Coronaviridae*, *Dicistroviridae*, *Flaviviridae*, *Hepeviridae*, *Orthomyxoviridae*, *Paramyxoviridae*, *Phenuiviridae*, *Picornaviridae, Pneumoviridae, Sedoreoviridae, Spinareoviridae, Togaviridae* and *Tobaniviridae*) and 24 species of DNA virus from four families (*Anelloviridae, Adenoviridae, Circoviridae* and *Parvoviridae*), some of which were present in high abundance (Fig. 2a, Extended Data Fig. 1). Members of the *Paramyxoviridae*, *Coronaviridae* and *Caliciviridae* families were the most abundant in lung samples, while members of the *Coronaviridae*, *Sedoreoviridae* and *Astroviridae* families were most abundant in the intestines (Fig. 2a).

These data greatly increased the diversity of virus families in multiple animal species: among the 125 viruses detected, over 60% led to an expansion in virus host range (Supplementary Fig. 1b). Most of the fur animal species sampled here contained between 2 and 23 vertebrate-associated virus species. Notably, mink carried 23 vertebrate-associated virus species from 11 viral families, raccoon dogs carried 19 virus species from 14 viral families, *Cavia porcellus* (guinea pig) carried 20 virus species from 11 viral families and Arctic foxes carried 13 virus species from six viral families (Fig.2b and Extended Data Figs. 1 and 2a). In the case of guinea pigs, we identified members of the *Flaviviridae*, *Circoviridae*, *Orthomyxoviridae*, *Pneumoviridae*, *Spinareoviridae* and *Parvoviridae* families for the first time, to our knowledge, in these animals (Extended Data Fig. 2b). Of the libraries that contained vertebrate-associated viruses, nearly half (n=166; 47.4%) contained 2–7 virus species (Fig. 2c (left)). Co-infections were most common in guinea pigs, mink, raccoon dogs and *Oryctolagus cuniculus* (the rex rabbit) (Fig.2c (right four panels)), including *Alphacoronavirus 1* and *Amdoparvovirus carnivoran 3*, as well as *Aichivirus A* with several Guinea pig astroviruses (Extended Data Fig. 2c). Two co-infection events involving *Rabbit coronavirus HKU14* (RbCoV HKU14) and rabbit coronavirus 1 were

observed in rabbits (Extended Data Fig. 2c). Approximately one-quarter of the genome sequences generated here were near complete and half were more than 93% complete, indicating a good coverage of viral genomes (Fig. 2d). Finally, no vertebrate-associated viruses were detected in 126 animals.

Evolutionary history and cross-species transmission of vertebrate-associated viruses

Phylogenetic analyses of the viruses identified here revealed a substantial diversity of vertebrate-associated viruses, some of evolutionary importance (Extended Data Figs. 3–6). The majority of viruses identified had relatively close evolutionary relationships to currently circulating viruses. However, more divergent lineages were also identified, such as a distinct member of the *Phenuiviridae* family in *Mustela sibirica* (Siberian weasel; weasel phenui-like virus), and a divergent member of the *Arteriviridae* family in *Sciurus vulgaris* (Eurasian red squirrel; squirrel arterivirus 1). In total, 36 virus species from 12 families were considered to be novel according to current species demarcation criteria by the International Committee on Taxonomy of Viruses (ICTV). These novel viruses mainly originated from the *Picornaviridae* (n=8), *Caliciviridae* (n=4) and *Circoviridae* (n=6), although novel viruses were also identified in virus families containing a high frequency of zoonotic viruses, such as the *Flaviviridae* and *Paramyxoviridae*, as well as in less common families such as *Adenoviridae*, *Anelloviridae*, *Phenuiviridae* and *Arteriviridae*.

We identified multiple viruses associated with human infection. For example, *Paslahepevirus balayani* (that is, hepatitis E virus (HEV); *Hepeviridae*) was detected in intestine samples from two rabbits and three raccoon dogs (two of which were wild) with 86.7%–94.0% genome identity, and belonging to the genotypes G3 and G4, which contain human-derived virus sequences. Notably, we identified Japanese encephalitis virus (JEV; *Flaviviridae*) in a rodent (guinea pig), with a sequence most closely related to swine and human-derived JEV in genotype G1 (98.6% and 96.4% genome identity, respectively; Extended Data Figs. 4a and 7). Mammalian orthoreovirus (mammalian reoviruses (MRV)) from the *Spinareoviridae* family was detected in Eurasian red squirrel (MRV2), raccoon dogs (MRV1 and MRV2), guinea pigs (MRV1) and mink (MRV3), with MRV2 and MRV3 associated with human infection. Several common human diarrhoeal pathogens were also documented, including four genotypes of norovirus (NV) in mink (GII, GIV and GVI), raccoon dogs (GVI) and foxes (GVII), among which GII and GIV are directly associated with human infection. Multiple genotypes of rotavirus A (RVA) were identified in 13 animal species, with the G3 genotype found in nine animal species (Extended Data Fig. 7). Moreover, rotavirus C (RVC), which mainly infects humans, pigs and cattle, was identified in an Arctic fox.

These data also revealed frequent cross-species transmission among animal viruses, involving transmission between wild and farmed animals. For example, *Getah virus* (GETV), which is mainly associated with livestock, including domestic pigs and horses, was identified in a raccoon dog (Extended Data Fig. 3). Similarly, murine pneumonia viruses (MPVs; *Pneumoviridae*) were identified in wild guinea pig and farmed raccoon dog, and were found to be closely related (98.7% and 95.6% genome identity, respectively) to viruses previously associated with hosts such as mice, dogs and pangolins. Many of these viruses also had a broad host spectrum, such as *Morbillivirus canis* (canine distemper virus (CDV);

Paramyxoviridae), which was identified in seven animal species from different regions of China, two of which were of wild origin. Potential cross-species transmission events of coronaviruses and IAVs were also frequently observed between farmed and wild animals (Extended Data Figs. 4b and 5).

Coronaviruses and IAVs in fur animals

Our metagenomic data provided evidence for seven coronavirus species in 66 farmed fur animals, greatly expanding the host range of these important emerging viruses. This included 20 Alphacoronavirus 1 viruses (specifically, canine coronavirus (CCoV)) in two host species: raccoon dogs and red foxes. Moreover, we identified Mink coronavirus 1 viruses in 18 mink, one Betacoronavirus 1 virus (that is, canine respiratory coronavirus) in a raccoon dog, 20 RbCoV HKU14-like viruses in guinea pigs and rabbits, and three China Rattus coronavirus HKU24-like viruses in *Myocastor coypus* (nutria) (Extended Data Fig. 5).

Of particular concern was the identification of *Pipistrellus* bat coronavirus HKU5-like viruses (subgenus *Merbecovirus*) in the lungs and intestines of two farmed mink. The mink HKU5-like CoVs form a lineage that is relatively closely related to viruses that were thus far reported only in bats, in which they have a history of recombination (Extended Data Fig. 8). Also of note was the identification of a novel CoV with a deletion in the HE protein (Supplementary Fig. 1c), tentatively named rabbit coronavirus 1, that fell within the subgenus *Embecovirus* alongside Pika coronavirus and Betacoronavirus 1. Finally, the very high frequency of divergent and abundant CoVs in the organs of these dead animals (for example, in 21 samples, CoVs reached abundance levels of 1.2×10^4 – 4.9×10^5 reads per million (RPM)) raises the question of whether they are directly responsible for the disease observed.

With respect to IAV, we identified two H5N6 viruses in two mink, one H1N2 virus in a guinea pig and a H6N2 virus in a muskrat. Time-scaled phylogenetic analysis indicated that, for most segments, the H1N2 virus descended from human H1N1/09 or closely related swine viruses (Extended Data Fig. 9), although, in four segments (PB1, NP, M and NS), it was most closely related to viruses found in swine (Extended Data Fig. 9). This suggests that the guinea pig H1N2 virus resulted from a reassortment event in swine after a reverse zoonosis event from humans. In addition to inheriting an N2 NA segment from swine H3N2 viruses through reassortment, the NS segment in the guinea pig H1N2 is related to a swine virus that is a sister swine lineage to human H1N1/09 (Extended Data Fig. 9). The two mink-derived H5N6 sequences were of the highly pathogenic (HPAI) phenotype, with high sequence similarity to viruses in avian or human hosts (Extended Data Fig. 10). The very recent ancestry (that is, 1 to 2 years before the sampling time of mink H5N6) was also apparent in the molecular clock analysis of all segments except for PB1. Phylogenetic analysis of the HA gene showed that it was a member of clade 2.3.4.4b (Extended Data Fig. 10) that has spread globally causing considerable concern. The mink virus also contained the D701N mutation in PB2 that has been associated with mammalian adaptation[30]. Finally, the H6N2 subtype in a muskrat (that is, rodent) represents, to our knowledge, the first identification of this subtype of avian influenza virus in mammals, with

the HA and NA segments exhibiting 96.8% and 97.0% nucleotide identity to viruses of avian origin (Eurasian lineage, ST/339-like subtype), respectively (Supplementary Fig. 1d).

Characteristics of viruses with high emergence potential

To identify viruses with an increased or high risk of cross-species transmission, we classified the viruses identified here according to whether they likely have the potential to jump species barriers between humans and animals or among animals. Accordingly, we identified 39 potentially high-risk viruses that had seemingly experienced frequent host jumping, including 11 zoonotic viruses (that is, previously found in humans), 15 cross-order viruses (not yet found in humans, but observed in two or more animal orders), and 13 potentially high-risk novel viruses (that is, the novel virus comes from a genus found in at least three mammalian orders) (Fig. 3a, Extended Data Fig. 11a). At the level of host order, the greatest number of risk viruses (n=21) were found in the *Carnivora*. RVA was identified in 13 species from four orders of fur animals, while IAV, MRV, and HEV were present in at least two mammalian orders (Figure 3a). Note that we detected *Pipistrellus* bat coronavirus HKU5 and RbCoV HKU14 in *Carnivora* and *Rodentia*, respectively, for the first time. Thus, these represent two cross-order viruses that may present a relatively high risk of emergence.

In total, 16 potentially high-risk viruses were detected in the intestines, 8 were detected in the lungs and 14 were detected in both tissues (Fig. 3a). After excluding animals with small sample sizes (that is, <5), we calculated the Gini-Simpson and Shannon richness indices for different animals. Eurasian red squirrels exhibited a higher diversity and richness of potentially high-risk viruses (Fig. 3b), while raccoon dogs carried up to ten potentially high-risk virus species, exceeding that of other animals. On the basis of the number of potentially high-risk virus species they carried, raccoon dogs (n=10, *Carnivora*), mink (n=10, *Carnivora*), guinea pigs (n=9, *Rodentia*), rabbits (n=6, *Lagomorpha*) and Arctic foxes (n=6, *Carnivora*), constituted potentially high-risk hosts for the transmission of viruses to humans and other animals.

Most (n=29) potentially high-risk viruses were sampled from east China, with a detection rate of 40.5%. Notably, 19 potentially high-risk viruses were detected in Shandong province, which contains many fur animal farms[31]. Several viruses showed both a wide geographical distribution and a broad host range. For example, RVA was detected in 13 species of fur animals in 14 provinces across seven regions of China, while CDV was detected in seven host species sampled in Hebei (North China), Henan (Central China), Jiangsu and Shandong (East China), Liaoning (Northeast China). By contrast, GETV, rabbit coronavirus 1 and JEV were detected only in Heilongjiang, Jiangsu and Guangxi provinces, respectively (Fig. 3c and Extended Data Fig. 11b).

Discussion

Farmed fur animals can act as reservoirs for zoonotic viruses[6,23,32]. We characterized the tissue-based vertebrate-associated virome of individual dead fur animals, some for the first time, to our knowledge, and many not previously studied at depth[33,34]. From this analysis, we identified 125 vertebrate-associated virus species from 20 virus families, and found that co-infection is commonplace. Importantly, this included 11 zoonotic viruses and 15 viruses

that exhibit transmission among mammalian orders. These viruses may be at heightened risk of emergence and should therefore be monitored closely. Overall, 13 novel virus species identified in this study belong to potentially high-risk viral genera. The order *Carnivora* carried the highest number of potentially high-risk viruses in this study, while guinea pigs (*Rodentia*) also carried a high diversity of viruses, including the first reports of JEV and IAV. Guinea pigs may therefore act as intermediate host in virus transmission chains and warrant more intensive surveillance.

The intensive breeding environment of farmed animals serves as a possible bridge for virus spillover. Indeed, we identified multiple viruses related to those that cause disease in humans and/or domestic animals, such as zoonotic MRV, IAV, HEV, NV, Betacoronavirus 1, Alphacoronavirus 1, RVA and RVC. The identification of NV in wild *Hydropotes inermis* (Chinese water deer) could indicate transmission from farmed animals. We detected viruses that were previously thought to be specific to particular host groups, such as MRV and MPV in guinea pigs, while RVA was found in the broadest set of hosts in this study, including *Capreolus pygargus* (Eastern roe deer), *Vicugna vicugna* (vicuna) and Chinese water deer, that were monitored for the first time. Our data also expanded the host range of zoonotic viruses, such as documenting JEV in guinea pigs, NV in mink, MRV in Eurasian red squirrels and multi-host pathogens such as GETV in a raccoon dog. These viruses have clear cross-species transmission potential. Moreover, we identified a variety of novel viruses, such as Guinea pig astroviruses. More regular surveillance of these animals—especially mink, raccoon dogs and guinea pigs, which had particularly rich viromes—is required to evaluate the potential risks to public health that stem from fur animal farming. There are a number of challenges in undertaking such expanded surveillance, especially in the case of multipurpose animals for which there is often a lack of reliable data on the size and distribution of breeding operations.

The high prevalence and diversity of coronaviruses and influenza viruses was of particular note, implying that farmed fur animals are important intermediate hosts or reservoirs for these viruses. We identified a MERS-like coronavirus—*Pipistrellus* bat coronavirus HKU5—in two mink from a single farm associated with an outbreak of pneumonia, as well as the first report, to our knowledge, of a coronavirus in nutria. This illustrates a cross-order transmission event from wildlife to farmed fur animals that are in close contact with humans. The high abundance of HKU5-like viruses in lung samples from dead mink (RPM = 7.8×10^4) with symptoms of pneumonia suggests that it may be the causative disease agent. Similarly, we detected both CCoV-1 and CCoV-2 in raccoon dogs in eight cities with a high (37%; 19/52) positivity rate. CCoV-2 has also been identified in human cases from Haiti and Malaysia[12,35,36], indicating that the raccoon dog CCoV identified may have zoonotic potential. Our study highlights the potential of these species to act as sentinels to monitor the emergence of novel CoVs, particularly owing to their relatively high densities and frequent interactions with humans.

Influenza viruses are a common cause of epidemics and pandemics in humans and other animal species. We identified novel H6N2 and H5N6 avian influenza viruses in farmed muskrats and mink, as well as a novel H1N2 IAV in lung samples of a captive wild guinea pig that were probably generated by a reassortment event in swine. There have been more

than 50 cases of human infection with H1N2 IAV worldwide, with a reassortment pattern similar to that observed here[37]. Similarly, there have been more than 80 reports of human infection with H5N6, of which 87.5% have a history of contact with animals, attesting to the possibility of transmission from animals to humans[38]. Finally, the detection of H6N2 in muskrat is the first report, to our knowledge, of this AIV subtype in mammals, underscoring the importance of monitoring this virus in diverse animal species.

In summary, this study provides important reference data for a deeper understanding of the viruses and fur animal hosts that may eventually cause infectious disease outbreaks, and that should therefore be subject to greater surveillance.

Limitations of this study

Although this is one of the largest virome study of fur animals undertaken thus far, it was necessarily based on opportunistic sampling at specific geographical locations and therefore cannot be considered to be a form of nationwide surveillance. Despite our sampling efforts, sample sizes were small in some cases, and the focus on dead animals necessarily means that we cannot provide information on the viruses that circulate in healthy farmed fur animals. Similarly, the concentration on respiratory and gastrointestinal symptoms, and therefore lung and intestine sampling, means that we cannot identify viruses that are present only in other tissues.

Materials and Methods

Sample collection and processing

China is one of the world's largest producers and consumers of fur. In 2016, its mink fur output was 26.16 million pieces, second only to Europe's total of 39.05 million pieces, while the production of fox and raccoon dog fur greatly exceeded that in other localities, reaching 12.65 million and 14.69 million pieces, respectively (https://www.actasia.org/). Four animal species are specifically farmed for the fur trade in China: silver foxes, Arctic foxes, mink and raccoon dogs (which can be considered to be the main fur animals). Some fur trading data for these species are publicly available (https://www.chinaleather.org/front/article/126301/), and their farming is largely concentrated in Hebei, Shandong, Heilongjiang and Liaoning provinces. Moreover, scattered, yet sometimes nationwide, breeding of other animal species also takes place (the "other" fur animals). The species that fall into this category include rabbit (specifically the rex rabbit strain), sika deer, roe deer, badger and muskrat, among others. These animals are not only bred for fur, but also for food and medicinal products, although systematic data on the scale and distribution of breeding is unavailable. In many cases, there is a lack of systematic record-keeping and supervision, with very little pathogen monitoring.

To study the virome of fur animals, we sampled diseased dead animals between 2021 and 2024 on the basis of three criteria: (i) the four main species of farmed fur animals were primarily sampled in their densely farmed provinces (that is, Hebei, Shandong, Heilongjiang and Liaoning), with sporadic collections in other provinces (Fig. 1); (ii) for the scattered, widely geographically distributed multiple-use animals, we performed a

nationwide sample collection; (iii) we collected wild-sourced samples from animal species that can sometimes be used for fur. In total, 461 animals were sampled, comprising 28 species from 5 mammalian orders. All dead animal sample collection was conducted by professional veterinary collaborators. The sampling and sample-processing procedures were approved by the ethics committee of Changchun Veterinary Research Institute, Chinese Academy of Agricultural Sciences (No. IACUC of AMMS-11–2020–012).

The collectors placed samples labelled with animal information onto dry ice for cryogenic transportation. After arrival at the laboratory, lung and intestinal samples were selected for further processing and research based on animal clinical records, concentrating on respiratory and gastrointestinal signs, while the remainder was stored long-term in a −80°C freezer. To confirm the identity of the host animal species sampled, the mitochondrial cytochrome B (*CytB*) gene was amplified and sequenced[39].

RNA extraction, library construction and sequencing

According to overall clinical symptoms and sample acquisition, we constructed single-tissue sample libraries from the lungs and intestines of animals sampled. In the case of the rare wild sika deer, for which only liver samples were preserved, a single liver sample was constructed. Total RNA extraction was conducted according to the manufacturer's instructions using the RNA Clean & Concentrator™-5 kit (Zymo Research). After depleting ribosomal RNA (rRNA) using the Ribo-Zero Plus rRNA Depletion Kit (Illumina) and TIANSeq rRNA Depletion Kit (TIANGEN Biotech), read libraries were constructed using the TruSeq Stranded mRNA Total Library Prep kit (Illumina) and sequenced on the Illumina Novaseq 6000 platform (150 bp paired-end).

Data processing and virus identification

Adapter and quality-trimming for all sequencing reads were performed using Trimmomatic (v0.39)[40]. Bowtie2 (v2.2.5) was used to map quality-controlled reads to the SILVA database (www.arb-silva.de, v132.1) with end-to-end parameters to remove reads related to rRNA[41]. We performed a *de novo* assembly of rRNA-free reads using MEGAHIT (v1.2.8) with the parameter --min-contig-len set to 300 bp[42]. For the assembled contigs, we used Diamond blastx to align them against the non-redundant protein database (accessed, 5 May 2023) with an *e*-value threshold of 1×10^{-6} [43]. Contigs with the top blast hit classified under the kingdom "Viruses" were preliminarily identified as viral sequences.

As our focus was on vertebrate-associated viruses, we filtered the data on the basis of annotated family and genus classification information to obtain viral contigs that are most likely associated with vertebrates (excluding the *Retroviridae*). Moreover, we focused on highly abundant viral genomes with relatively high similarity to known viruses and did not mine beyond this. The species assignment of the viral sequences obtained was performed using species demarcation criteria established by the International Committee on Taxonomy of Viruses for each virus genus. For genera that lacked clear species demarcation criteria, a relatively conservative threshold of 80% amino acid identity in the RNA-dependent RNA polymerase (RdRp) or replicase to known virus species was applied. Detailed information on the species demarcation criteria used is provided in Supplementary Table 1. For the

sequences of the vertebrate-associated viruses obtained, we designed a series of specific primers and used PCR or RT-PCR for validation and filling gaps in incomplete virus genome. Furthermore, we used RACE kits to obtain the terminal ends of the viral genomes.

Viral abundance based on transcriptome data

To quantify the abundance of vertebrate-associated viruses, we mapped the rRNA-free reads to the putative virus genomes identified above implemented in Bowtie2 (v2.2.5), resulting in read count calculations for each virus. Virus abundance was represented as the number of reads mapped per million (RPM). To reduce false-positive virus discovery, only viruses with a threshold of RPM ≥ 1 and verified by PCR were included. Data processing and visualization was implemented in R (v 4.2.1), using multiple packages (*Pheatmap*, *ggplot2*, *tidyverse*, *PieGlyph*, *svglite*, *vegan*, *picante*, *ggalt*, *sankeywheel*, *ggalluvial*)[44,45].

Sequence alignment, phylogenetic analyses and recombination detection

To estimate phylogenetic trees for each of the vertebrate-associated viruses documented here, we used amino acid sequences of hallmark viral proteins, namely RdRp for RNA viruses and the DNA polymerase for DNA viruses (some viral sequences were not included in the phylogenetic analysis due to a lack of RdRp sequences). We individually aligned the amino acid sequences of each virus family using the L-INS-i algorithm in MAFFT (v7.402)[46] and trimmed ambiguously aligned regions with trimAl (v1.2)[47]. Finally, we manually inspected the sequences in MEGA11[48]. Recombination analysis was performed using Simplot and Splitstree5[49,50]. We estimated maximum likelihood (ML) trees for each virus family using IQ-TREE (v2.1.4)[51]. Similarly, we used IQ-TREE to infer ML trees for some representative virus species. IQ-TREE's built-in ModelFinder was used to select the optimal model of amino acid/nucleotide substitution in each case. For particular coronaviruses (CoVs) and influenza viruses, we estimated time-calibrated trees using BEAST (v1.10.5)[52] and summarized them as maximum clade credibility trees. These analyses were performed using codon-position partitioning, a general time-reversible nucleotide substitution model with gamma-distributed rate variation among sites (GTR+Γ) for each position[53,54], an uncorrelated relaxed clock model and a flexible Skygrid coalescent tree prior[55]. For each genome segment, a sufficient number of iterations was used to ensure that effective sample sizes were >200.

Definition and identification of viruses with high emergence potential

The host ranges of viruses from the NCBI/GenBank were collected and organized (on the basis of data available in November 2023). We categorized three types of potentially high-risk viruses: (i) a *zoonotic* virus was defined as a virus that has been found at least once in humans; (ii) a *cross-order* virus was defined as a virus that has not yet been reported to infect humans, but which has been found in two or more animal orders; (iii) a *novel potential risk* virus was defined as a virus with >60% amino acid similarity to known viruses, where the genus in question has been found in more than three mammalian orders (that is, as there are necessarily no previous reports for the novel viruses identified in this study, we made judgments on the basis of the virus genus to which these viruses belong).

Extended Data

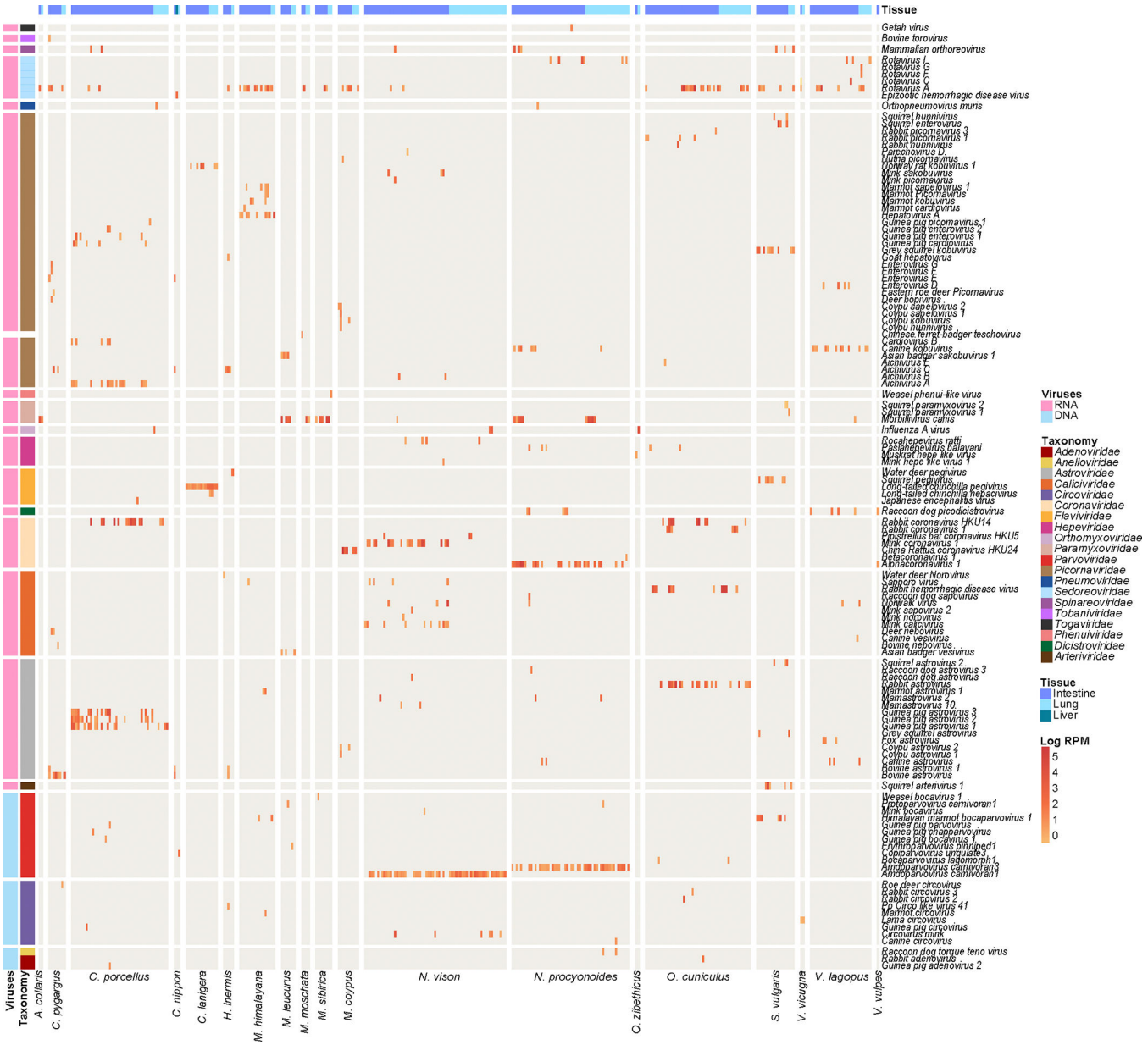

Extended Data Figure 1. Abundance of vertebrate-associated viruses in fur animals at the species level.

The abundance of each virus was calculated and normalized based on the number of mapped reads per million total reads (RPM) and presented on the Log-10 scale. Different colour blocks represent different types of viruses and source organs. Source data are provided in the Source Data file.

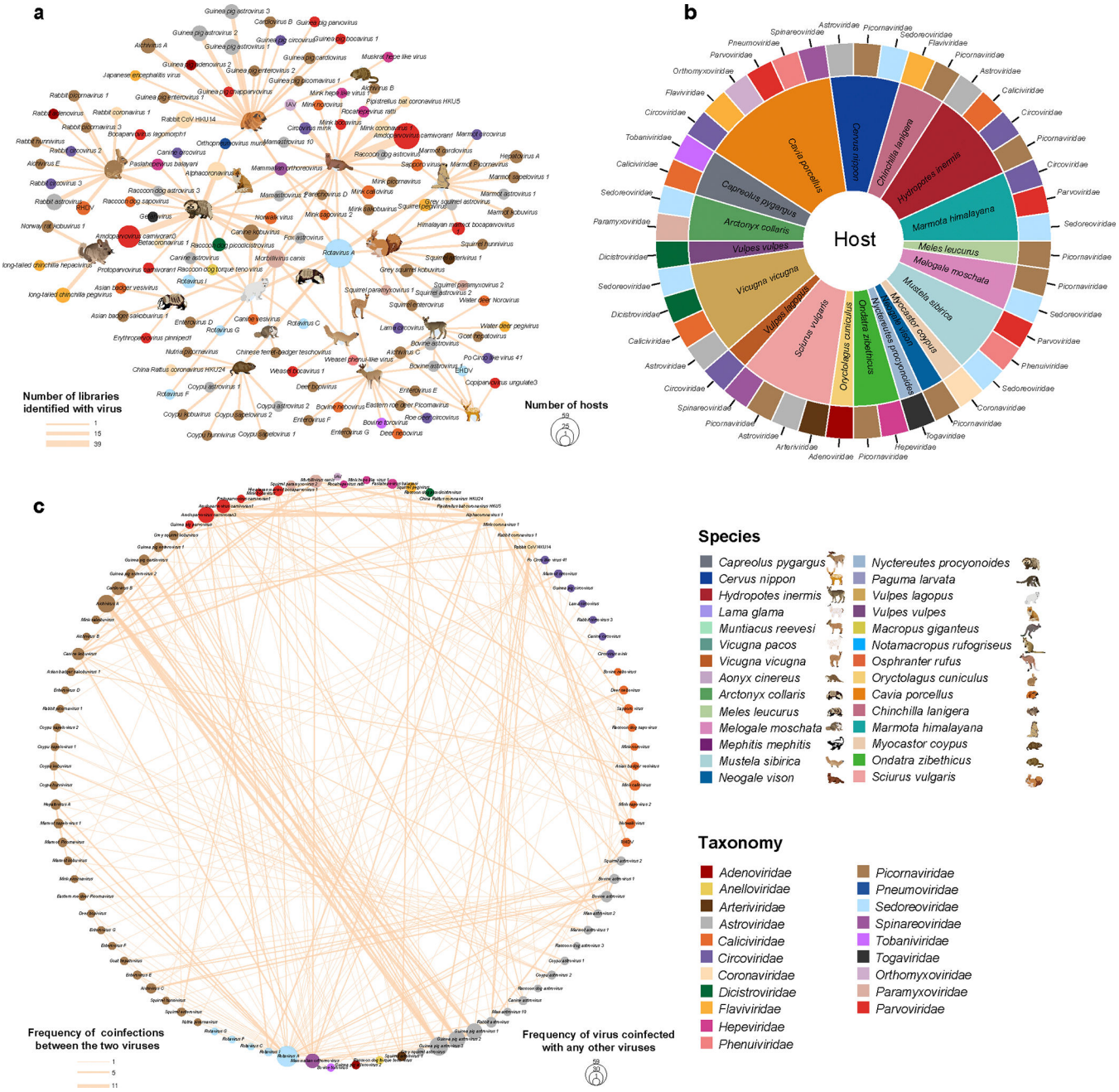

Extended Data Figure 2. Newly discovered viruses, the infection spectrum of the animals studied and the extent of coinfection.

(a) The infection spectrum of the studied animals, with animals represented by images. Viruses are shown at the nodes, with the node colour specifying the viral family. The size of the nodes represents the number of animals infected by the virus, and the width of the edges indicates the number of libraries of the host infected by the connected virus. (b) The viral families newly identified in the specific host. Each segment of the pie chart corresponds to a distinct animal species, depicted with unique colour, and the donuts with similar lighter colour, signify the newly discovered viral families. (c) Virus co-infection.

Viruses are shown at the nodes, with the node colour specifying the viral family. The size of the nodes represents the frequency of co-infections with any other virus, while edge width represents the frequency of co-infections between the two viruses.

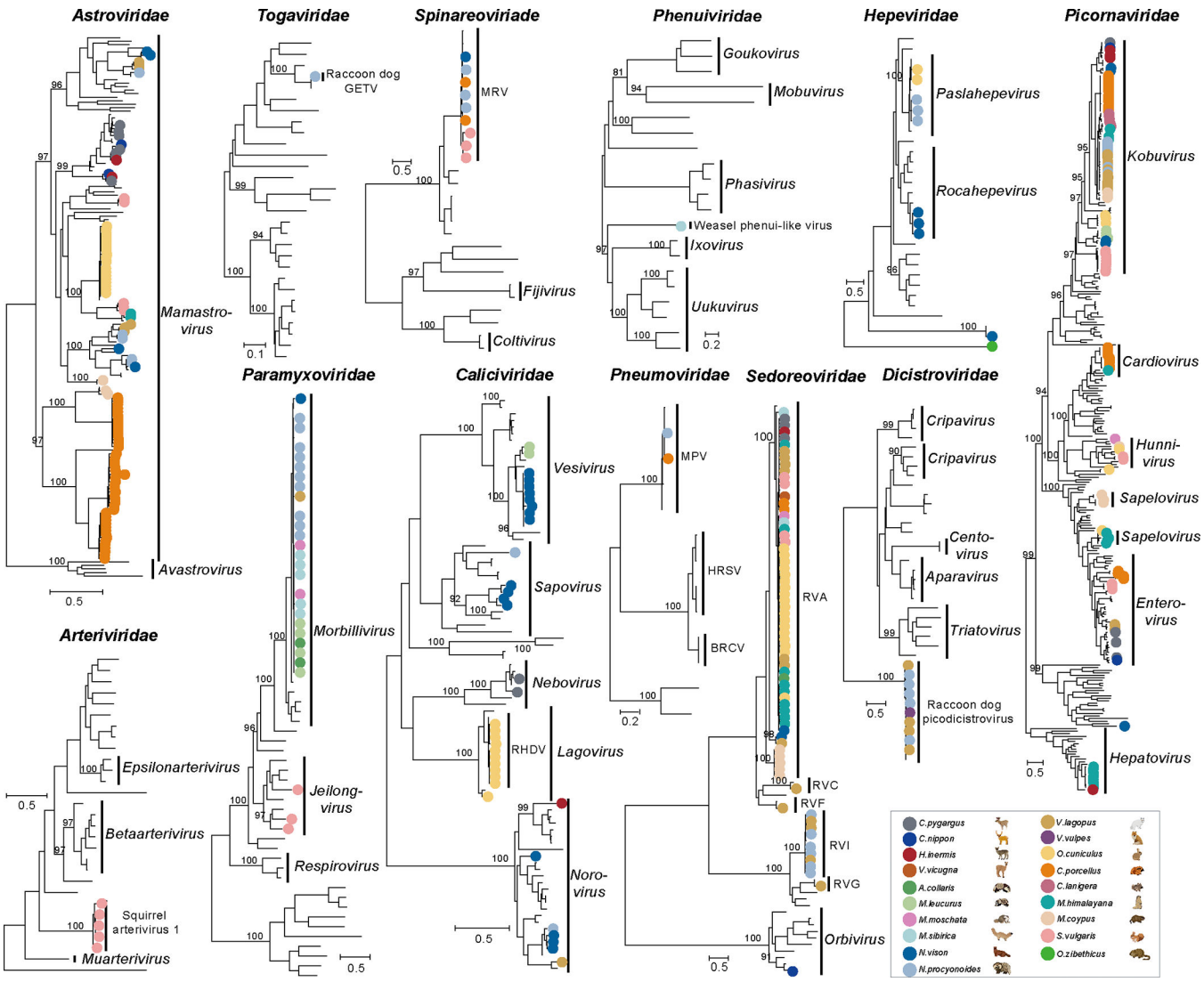

Extended Data Figure 3. Inter-specific phylogenetic trees of 12 major families of vertebrate-associated RNA viruses.

Phylogenetic trees were inferred for each family of RNA viruses based on amino acid sequences of the RNA-dependent RNA polymerase protein. All trees are midpoint-rooted for clarity and display bootstrap values for major branches. Coloured dots represent viruses with different host origins. The scale bar represents the number of amino acid substitutions per site.

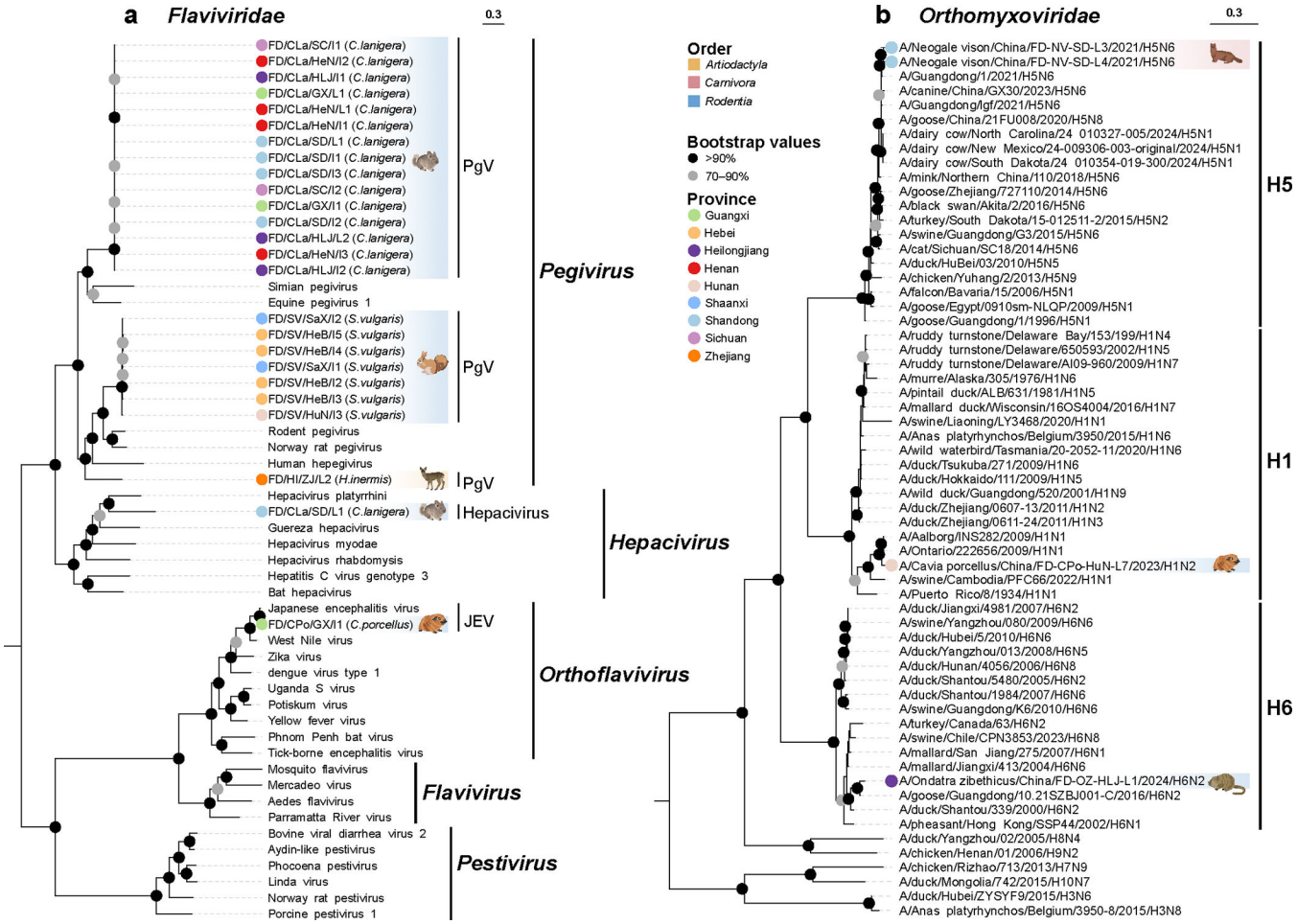

Extended Data Figure 4. Phylogenetic trees of vertebrate-associated RNA viruses from the Flaviviridae and Orthomyxoviridae in fur animals.

Phylogenetic trees of viruses in the (a) *Flaviviridae* and (b) *Orthomyxoviridae* were inferred from the amino acid sequences of the RNA-dependent RNA polymerase and hemagglutinin proteins (*Orthomyxoviridae*). All trees are midpoint-rooted for clarity and display bootstrap values for major branches. Different coloured dots represent viruses with different geographic origins. Colour shading represents different animal orders, and specific species are depicted with animal pictures. The scale bar represents the number of amino acid substitutions per site.

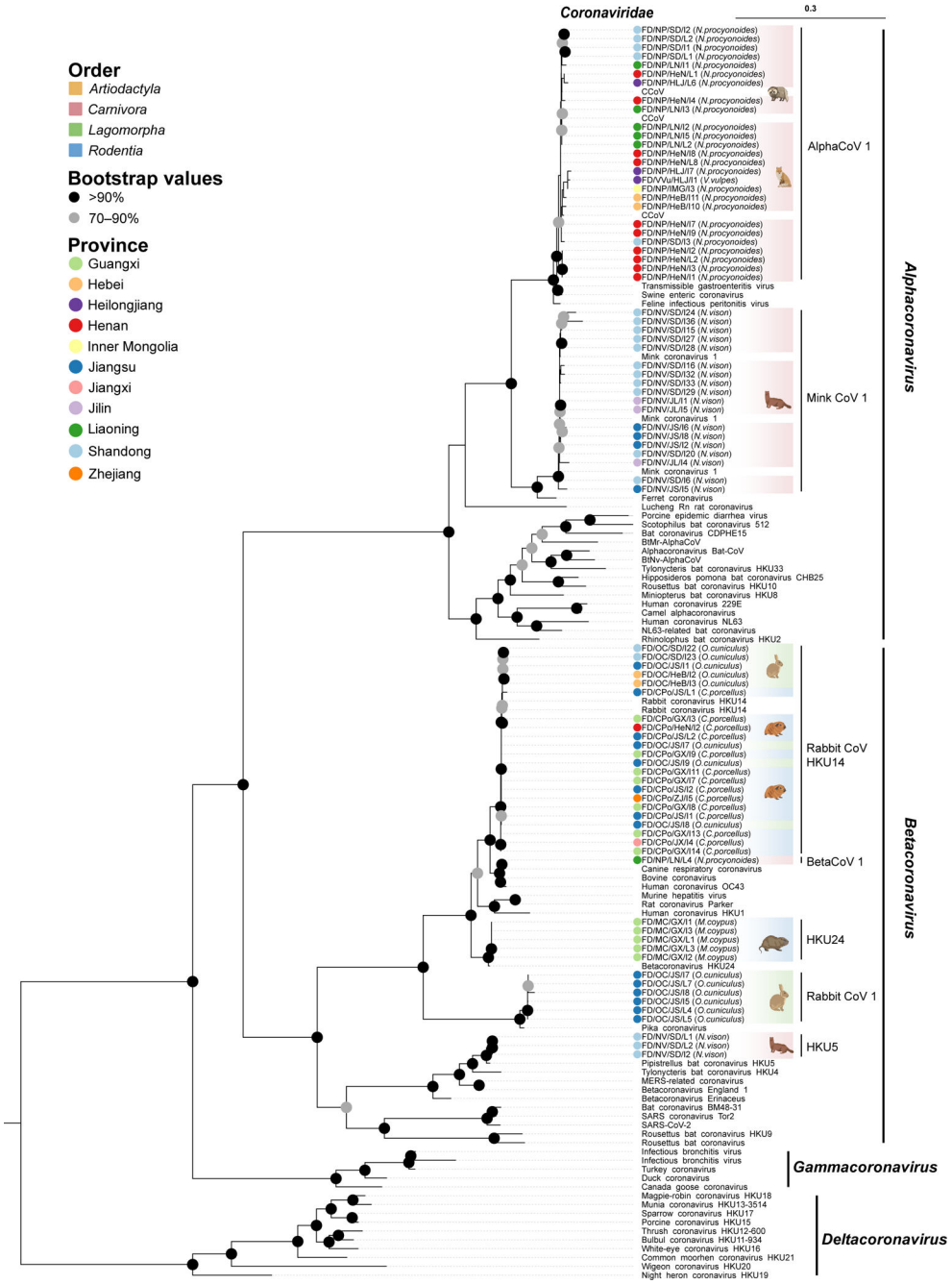

Extended Data Figure 5. Phylogenetic tree of the Coronaviridae in farmed animals.

Phylogenetic tree of viruses in the *Coronaviridae* inferred from the amino acid sequences of the RNA-dependent RNA polymerase. The tree is midpoint-rooted for clarity and displays bootstrap values at the major branches. Different coloured dots represent viruses with different geographic origins. Colour shading represents different animal orders, and specific species are depicted with animal pictures. The scale bar represents the number of amino acid substitutions per site.

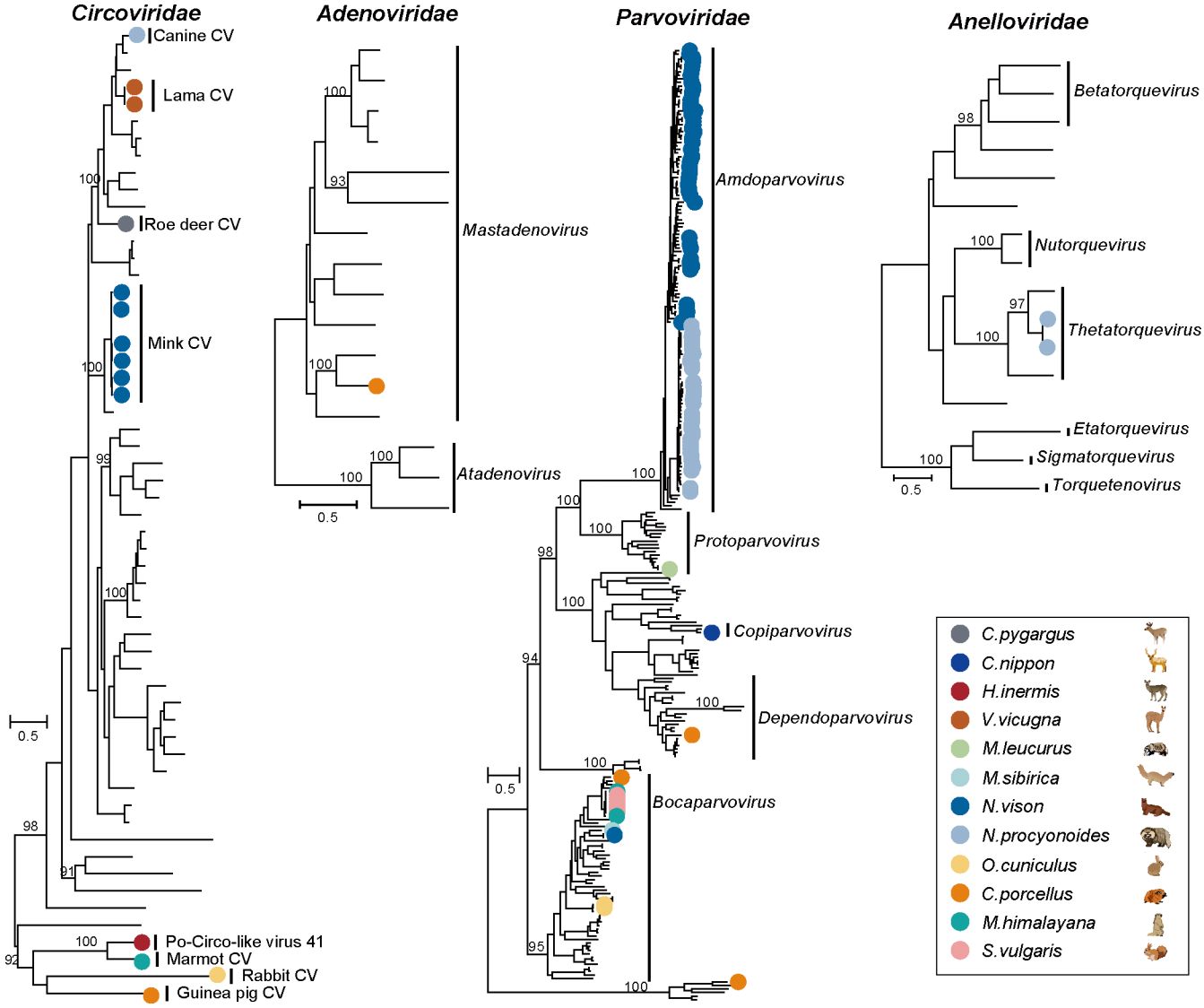

Extended Data Figure 6. Inter-specific phylogenetic trees of four vertebrate-associated DNA virus families.

Phylogenetic trees were inferred for each DNA virus family based on the amino acid sequences of conserved viral proteins (DNA viruses = replication related protein, i.e., *Anelloviridae*: ORF1, *Parvoviridae*: NS1, *Adenoviridae*: DNA polymerase, and *Circoviridae*: Rep protein). All trees are midpoint-rooted for clarity and display bootstrap values for major branches. Coloured dots represent viruses with different host origins. The scale bar represents the number of amino acid substitutions per site.

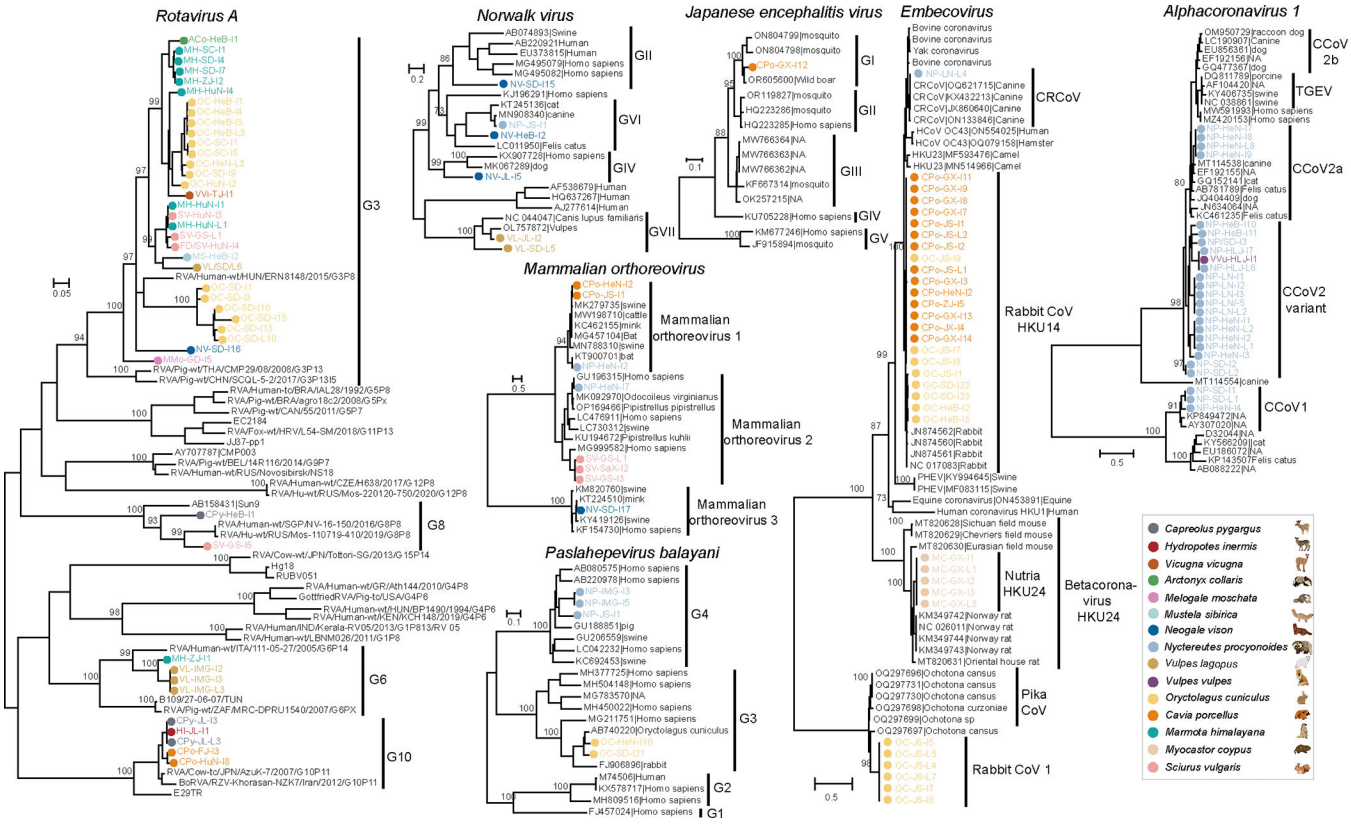

Extended Data Figure 7. Intra-specific phylogenetic diversity of multi-host infecting viruses identified in fur animals.

Phylogenetic trees were inferred for each virus species based on the nucleotide sequences of the key gene (i.e., Coronavirus: S1 gene, *Paslahepevirus balayani*: full genome, Japanese encephalitis virus: E gene, Mammalian orthoreovirus: S1 gene, Norwalk virus: VP1, Rotavirus A: VP7). All trees are midpoint-rooted for clarity and display bootstrap values for the major branches. Coloured dots represent different host sources.

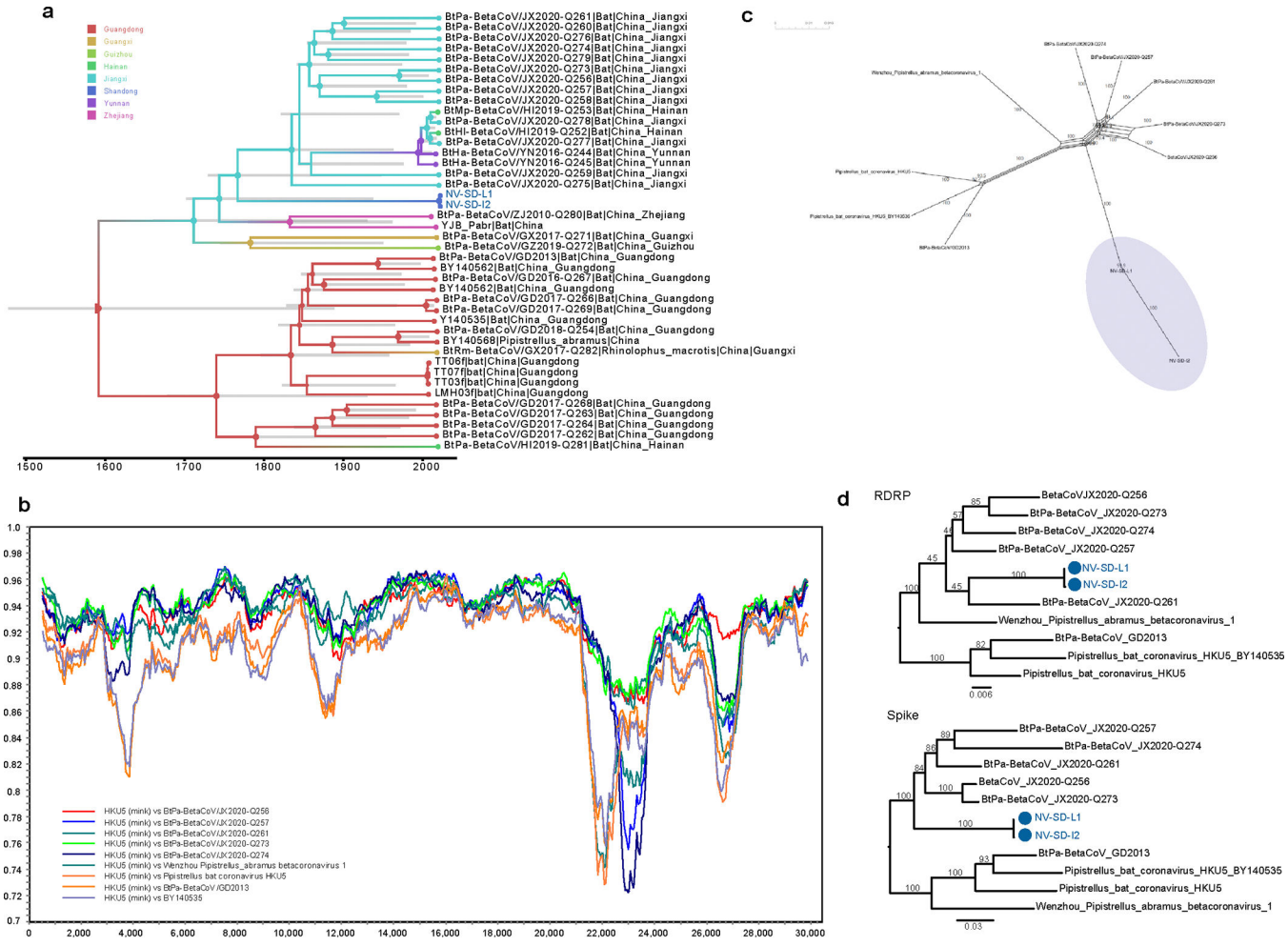

Extended Data Figure 8. Recombination and phylogenetic analysis of mink-derived Pipistrellus bat coronavirus HKU5.

(a) Maximum clade credibility (MCC) tree based on genome of mink-derived HKU5-like viruses. (b) Simplot was used to perform recombination scanning on the mink-derived HKU5-like sequences and related reference sequences. (c) Neighbor-Net reconstruction based on the complete genome sequences of mink HKU5 and Bat CoVs using Splitstree5, employing the HKY85 substitution model and 1000 bootstraps. (d) IQ-TREE (v2.1.4) was used to estimate maximum likelihood trees based on RdRp and S gene nucleotides, respectively.

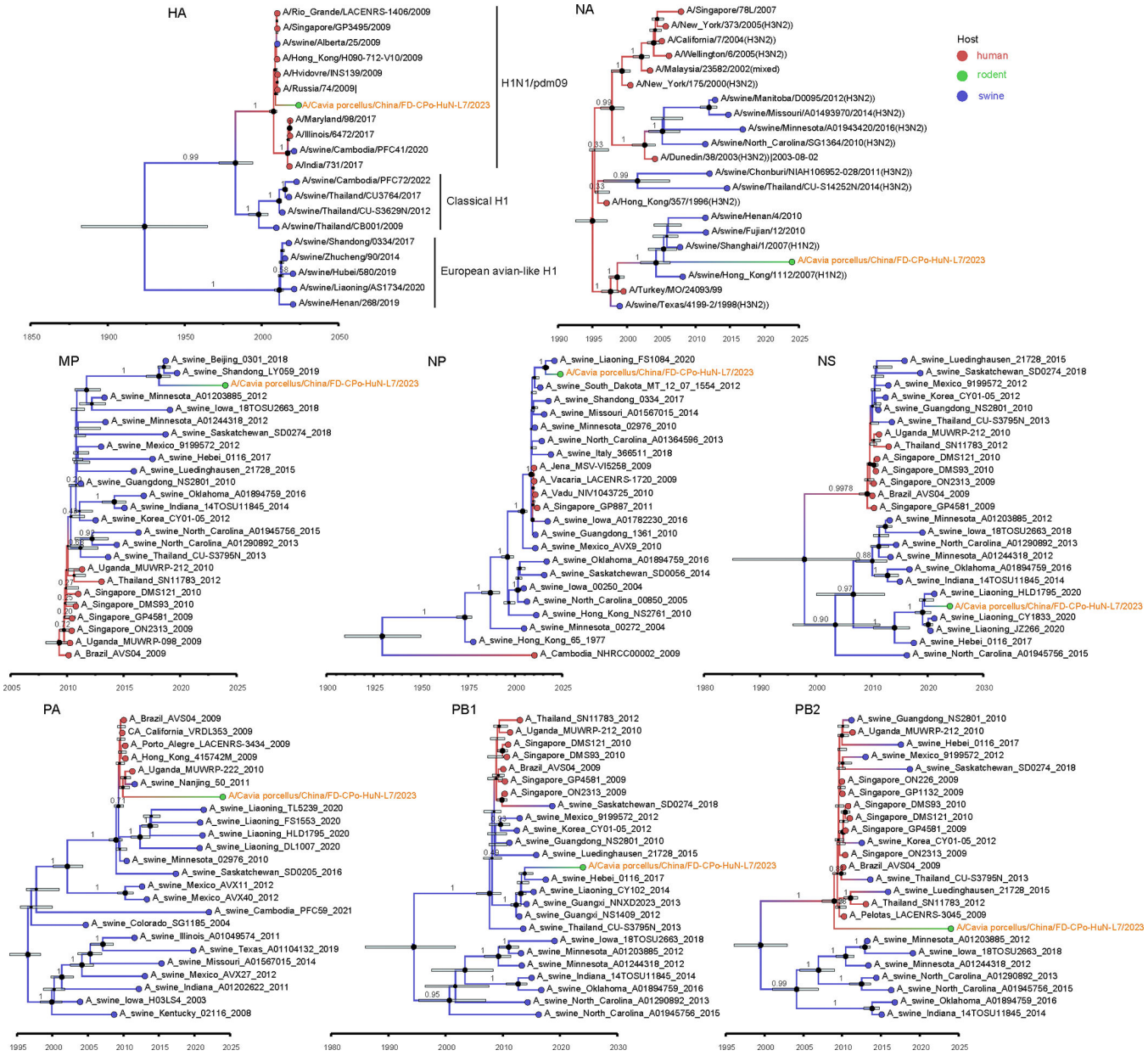

Extended Data Figure 9. Phylogenetic analysis of guinea pig-derived Influenza A virus H1N2. Maximum clade credibility (MCC) trees based on the HA, MP, NA, NP, NS, PA, PB1, and PB2 gene sequences of H1N2 influenza virus. MCC trees were summarized from Bayesian phylodynamic inferences using BEAST (v1.10.5). Coloured lines and dots represent the host: human (red), rodent (green), and swine (light-blue).

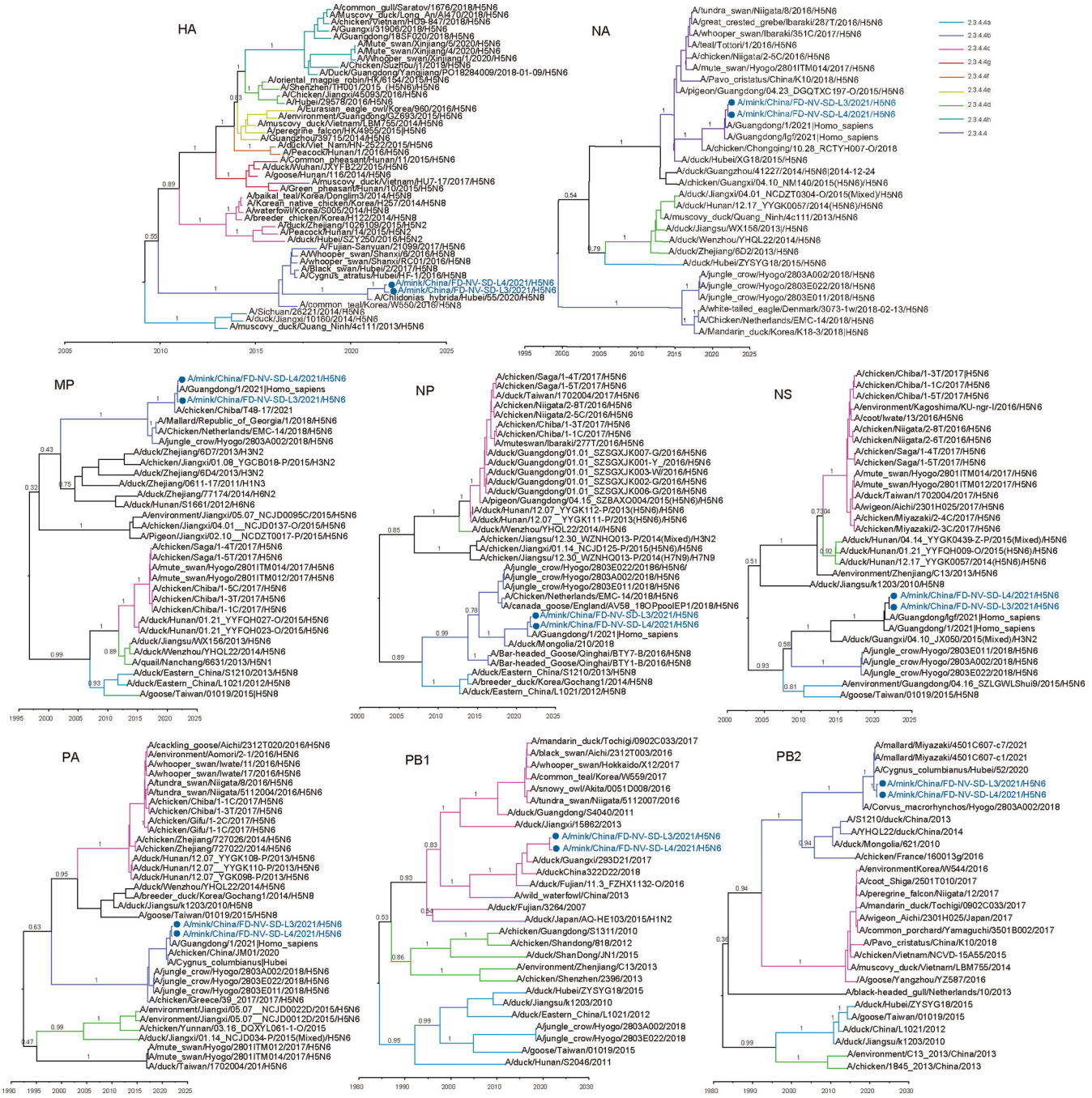

Extended Data Figure 10. Phylogenetic analysis of two mink-derived Influenza A virus H5N6.
Maximum clade credibility (MCC) trees based on the HA, MP, NA, NP, NS, PA, PB1, and PB2 gene sequences of H5N6. MCC trees were summarized from Bayesian phylodynamic inferences using BEAST (v1.10.5). Different virus clades are depicted in different colours. Blue dots denote the mink-derived H5N6 virus reported here.

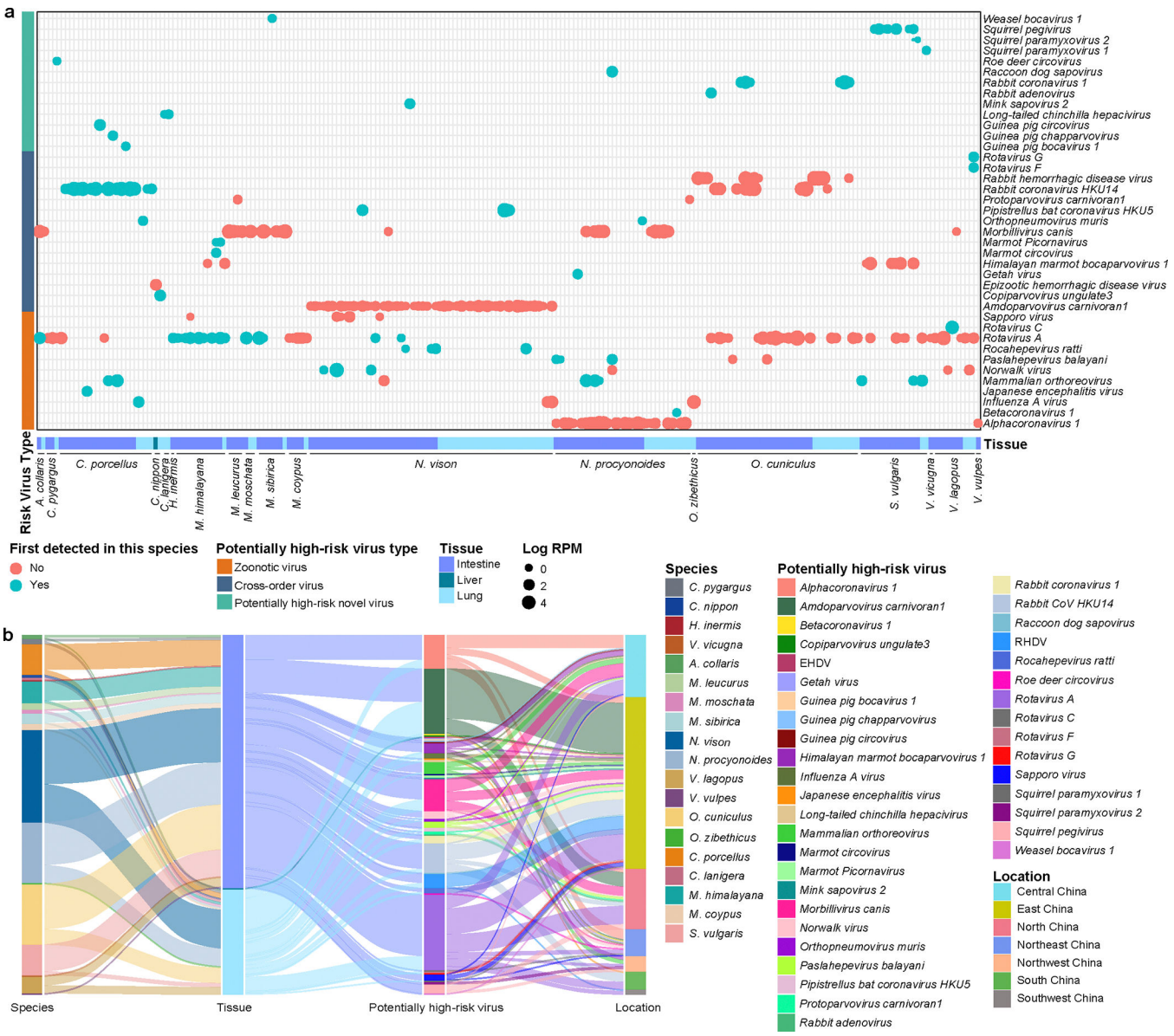

Extended Data Figure 11. Types and abundances of potentially high-risk viruses, along with their geographic and host origins

(a) The radius of the bubbles indicates the abundance of each potentially high-risk virus, with larger bubbles representing greater abundance. Green bubbles indicate that the virus was identified for the first time in the corresponding host species, while red bubbles indicate previous identification in that host. (b) The relationship between potentially high-risk viruses and their hosts, tissue types, and geographical regions. The line thickness represents the frequency.

Supplementary Material

Refer to Web version on PubMed Central for supplementary material.

Acknowledgments

S.S., J.Z., W. W., K.Y., M.L., Z.C., Y.L. and A.H. are financially supported by the National Key Research and Development Program of China (grant no. 2021YFD1801101), the Program of Shanghai Academic Research Leader (23XD1420700), the Young Top-Notch Talents of National Ten Thousand Talent Program. W.T.H. and G.Y. are support by Young Elite Scientists Sponsorship Program by CAST (2023QNRC001). PL and MAS are partially supported by US National Institutes of Health grant R01 AI153044. J.H.O.P is supported by the Swedish research council Vetenskapsrådet (grant no: 2020-02593). E.H. is supported by a National Health and Medical Research Council (NHMRC) Investigator award (GNT2017197) and by AIR@InnoHK administered by the Innovation and Technology Commission, Hong Kong Special Administrative Region, China. We gratefully acknowledge support from Advanced Micro Devices, Inc. with the donation of parallel computing resources through their AMD HPC Fund used for this research. The Y.B. laboratory involved in collecting and handling some samples of potential high-risk viruses, such as the HKU5-COV and H5N6 IAV, in accordance with regulations (approved by the Ethics Committee of the Institute of Microbiology, Chinese Academy of Sciences, approval number, HP-SQIMCAS2024111), and was financially supported by the National Key Research and Development Program of China (2021YFC2300903). S.S. (alternative email: ssh5658485@163.com) is the lead contact for this paper..

Data availability statement

The data reported in this paper have been deposited in the GenBase of the National Genomics Data Center, Beijing Institute of Genomics, Chinese Academy of Sciences/China National Center for Bioinformation (CNCB) under accession numbers C_AA074934.1 to C_AA076255.1. These data are publicly accessible online (https://ngdc.cncb.ac.cn/genbase). The raw sequencing read data have been deposited at the Genome Sequence Archive (Genomics, Proteomics & Bioinformatics 2021) of CNCB under the BioProject accession number PRJCA026706. The sequences of four IAVs have been submitted to the GISAID database, and assigned isolate IDs EPI_ISL_19176289, EPI_ISL_19176290, EPI_ISL_19176291, and EPI_ISL_19176294. All multiple-sequence alignments (fasta format), phylogenetic trees and source data related to figures in the main text have been deposited at GitHub (https://github.com/Jin2024-doct/-fur-animals-virus-dataset.git). The map of China is available from the Data Center for Resources and Environmental Sciences at the Chinese Academy of Sciences (http://www.resdc.cn). Source data are provided with this paper.

References

1. Lindh E et al. Highly pathogenic avian influenza A(H5N1) virus infection on multiple fur farms in the South and Central Ostrobothnia regions of Finland, July 2023. Euro surveillance : bulletin Europeen sur les maladies transmissibles = European communicable disease bulletin 28, doi:10.2807/1560-7917.Es.2023.28.31.2300400 (2023).
2. Enserink M Coronavirus rips through Dutch mink farms, triggering culls. Science (New York, N.Y.) 368, 1169, doi:10.1126/science.368.6496.1169 (2020). [PubMed: 32527808]
3. Peacock TP & Barclay WS Mink farming poses risks for future viral pandemics. Proceedings of the National Academy of Sciences of the United States of America 120, e2303408120, doi:10.1073/pnas.2303408120 (2023). [PubMed: 37467264]
4. Waller C et al. Japanese Encephalitis in Australia - A Sentinel Case. The New England journal of medicine 387, 661–662, doi:10.1056/NEJMc2207004 (2022). [PubMed: 36070717]
5. Eledge MR, Zita MD & Boehme KW Reovirus: Friend and Foe. Current clinical microbiology reports 6, 132–138, doi:10.1007/s40588-019-00121-8 (2019). [PubMed: 33134034]
6. Sabir JS et al. Co-circulation of three camel coronavirus species and recombination of MERS-CoVs in Saudi Arabia. Science (New York, N.Y.) 351, 81–84, doi:10.1126/science.aac8608 (2016). [PubMed: 26678874]

7. Woolhouse M & Gaunt E Ecological origins of novel human pathogens. Critical reviews in microbiology 33, 231–242, doi:10.1080/10408410701647560 (2007). [PubMed: 18033594]
8. Taylor LH, Latham SM & Woolhouse ME Risk factors for human disease emergence. Philosophical transactions of the Royal Society of London. Series B, Biological sciences 356, 983–989, doi:10.1098/rstb.2001.0888 (2001). [PubMed: 11516376]
9. Weingartl HM et al. Genetic and pathobiologic characterization of pandemic H1N1 2009 influenza viruses from a naturally infected swine herd. Journal of virology 84, 2245–2256, doi:10.1128/jvi.02118-09 (2010). [PubMed: 20015998]
10. Lu M et al. Zoonotic risk assessment among farmed mammals. Cell 186, 2040–2040.e2041, doi:10.1016/j.cell.2023.04.002 (2023). [PubMed: 37116474]
11. He WT et al. Virome characterization of game animals in China reveals a spectrum of emerging pathogens. Cell 185, 1117–1129.e1118, doi:10.1016/j.cell.2022.02.014 (2022). [PubMed: 35298912]
12. Vlasova AN et al. Novel Canine Coronavirus Isolated from a Hospitalized Patient With Pneumonia in East Malaysia. Clinical infectious diseases : an official publication of the Infectious Diseases Society of America 74, 446–454, doi:10.1093/cid/ciab456 (2022). [PubMed: 34013321]
13. Lednicky JA et al. Independent infections of porcine deltacoronavirus among Haitian children. Nature 600, 133–137, doi:10.1038/s41586-021-04111-z (2021). [PubMed: 34789872]
14. Agüero M et al. Highly pathogenic avian influenza A(H5N1) virus infection in farmed minks, Spain, October 2022. Euro surveillance : bulletin Europeen sur les maladies transmissibles = European communicable disease bulletin 28, doi:10.2807/1560-7917.Es.2023.28.3.2300001 (2023).
15. Conroy G Nipah virus outbreak: what scientists know so far. Nature, doi:10.1038/d41586-023-02967-x (2023).
16. Chua KB et al. Isolation of Nipah virus from Malaysian Island flying-foxes. Microbes and infection 4, 145–151, doi:10.1016/s1286-4579(01)01522-2 (2002). [PubMed: 11880045]
17. Miller RS et al. Cross-species transmission potential between wild pigs, livestock, poultry, wildlife, and humans: implications for disease risk management in North America. Scientific Reports 7, 7821, doi:10.1038/s41598-017-07336-z (2017). [PubMed: 28798293]
18. Magouras I et al. Emerging Zoonotic Diseases: Should We Rethink the Animal–Human Interface? Frontiers in Veterinary Science 7, doi:10.3389/fvets.2020.582743 (2020).
19. Johnson CK et al. Global shifts in mammalian population trends reveal key predictors of virus spillover risk. Proceedings of the Royal Society B: Biological Sciences 287, 20192736, doi:doi:10.1098/rspb.2019.2736 (2020).
20. Guan Y et al. Isolation and characterization of viruses related to the SARS coronavirus from animals in southern China. Science (New York, N.Y.) 302, 276–278, doi:10.1126/science.1087139 (2003). [PubMed: 12958366]
21. Hiono T et al. Virological, pathological, and glycovirological investigations of an Ezo red fox and a tanuki naturally infected with H5N1 high pathogenicity avian influenza viruses in Hokkaido, Japan. Virology 578, 35–44, doi:10.1016/j.virol.2022.11.008 (2023). [PubMed: 36462496]
22. Rijks JM et al. Highly Pathogenic Avian Influenza A(H5N1) Virus in Wild Red Foxes, the Netherlands, 2021. Emerging infectious diseases 27, 2960–2962, doi:10.3201/eid2711.211281 (2021). [PubMed: 34670656]
23. Oude Munnink BB et al. Transmission of SARS-CoV-2 on mink farms between humans and mink and back to humans. Science (New York, N.Y.) 371, 172–177, doi:10.1126/science.abe5901 (2021). [PubMed: 33172935]
24. Chen YM et al. Host traits shape virome composition and virus transmission in wild small mammals. Cell 186, 4662–4675.e4612, doi:10.1016/j.cell.2023.08.029 (2023). [PubMed: 37734372]
25. Xie XT, Kropinski AM, Tapscott B, Weese JS & Turner PV Prevalence of fecal viruses and bacteriophage in Canadian farmed mink (Neovison vison). MicrobiologyOpen 8, e00622, doi:10.1002/mbo3.622 (2019). [PubMed: 29635866]
26. Bodewes R et al. Viral metagenomic analysis of feces of wild small carnivores. Virology journal 11, 89, doi:10.1186/1743-422x-11-89 (2014). [PubMed: 24886057]

27. Zhang W et al. Virome comparisons in wild-diseased and healthy captive giant pandas. Microbiome 5, 90, doi:10.1186/s40168-017-0308-0 (2017). [PubMed: 28780905]
28. Fenollar F et al. Mink, SARS-CoV-2, and the Human-Animal Interface. Frontiers in microbiology 12, 663815, doi:10.3389/fmicb.2021.663815 (2021). [PubMed: 33868218]
29. Ahn H-S et al. Prevalence and genetic features of rabbit hepatitis E virus in Korea. Journal of Medical Virology 89, 1995–2002, doi:10.1002/jmv.24875 (2017). [PubMed: 28617964]
30. Czudai-Matwich V, Otte A, Matrosovich M, Gabriel G & Klenk HD PB2 mutations D701N and S714R promote adaptation of an influenza H5N1 virus to a mammalian host. Journal of virology 88, 8735–8742, doi:10.1128/jvi.00422-14 (2014). [PubMed: 24899203]
31. Wang W et al. Divergent Cryptosporidium species and host-adapted Cryptosporidium canis subtypes in farmed minks, raccoon dogs and foxes in Shandong, China. Frontiers in cellular and infection microbiology 12, 980917, doi:10.3389/fcimb.2022.980917 (2022). [PubMed: 36072226]
32. Cui J, Li F & Shi ZL Origin and evolution of pathogenic coronaviruses. Nature reviews. Microbiology 17, 181–192, doi:10.1038/s41579-018-0118-9 (2019). [PubMed: 30531947]
33. Yang S et al. Viral Metagenomics Reveals Diverse Viruses in the Feces Samples of Raccoon Dogs. Front Vet Sci 8, 693564, doi:10.3389/fvets.2021.693564 (2021). [PubMed: 34322538]
34. Lojkić I et al. Faecal virome of red foxes from peri-urban areas. Comparative immunology, microbiology and infectious diseases 45, 10–15, doi:10.1016/j.cimid.2016.01.005 (2016). [PubMed: 27012914]
35. Tortorici MA et al. Structure, receptor recognition, and antigenicity of the human coronavirus CCoV-HuPn-2018 spike glycoprotein. Cell 185, 2279–2291.e2217, doi:10.1016/j.cell.2022.05.019 (2022). [PubMed: 35700730]
36. Lednicky JA et al. Isolation of a Novel Recombinant Canine Coronavirus From a Visitor to Haiti: Further Evidence of Transmission of Coronaviruses of Zoonotic Origin to Humans. Clinical infectious diseases : an official publication of the Infectious Diseases Society of America 75, e1184–e1187, doi:10.1093/cid/ciab924 (2022). [PubMed: 34718467]
37. Sah R, Mohanty A, Rohilla R & Padhi BK A recent outbreak of human H1N2 infection: correspondence. International journal of surgery (London, England) 109, 604–605, doi:10.1097/js9.0000000000000185 (2023). [PubMed: 36906742]
38. Szablewski CM et al. Reported Global Avian Influenza Detections Among Humans and Animals During 2013–2022: Comprehensive Review and Analysis of Available Surveillance Data. JMIR Public Health Surveill 9, e46383, doi:10.2196/46383 (2023). [PubMed: 37651182]

References

39. Guillén-Servent A & Francis CM A new species of bat of the Hipposideros bicolor group (Chiroptera: Hipposideridae) from Central Laos, with evidence of convergent evolution with Sundaic taxa. Acta Chiropterologica 8, 39–61, doi:10.3161/1733-5329(2006)8[39:Ansobo]2.0.Co;2 (2006).
40. Bolger AM, Lohse M & Usadel B Trimmomatic: a flexible trimmer for Illumina sequence data. Bioinformatics (Oxford, England) 30, 2114–2120, doi:10.1093/bioinformatics/btu170 (2014). [PubMed: 24695404]
41. Langmead B & Salzberg SL Fast gapped-read alignment with Bowtie 2. Nature methods 9, 357–359, doi:10.1038/nmeth.1923 (2012). [PubMed: 22388286]
42. Li D, Liu CM, Luo R, Sadakane K & Lam TW MEGAHIT: an ultra-fast single-node solution for large and complex metagenomics assembly via succinct de Bruijn graph. Bioinformatics (Oxford, England) 31, 1674–1676, doi:10.1093/bioinformatics/btv033 (2015). [PubMed: 25609793]
43. Buchfink B, Xie C & Huson DH Fast and sensitive protein alignment using DIAMOND. Nature methods 12, 59–60, doi:10.1038/nmeth.3176 (2015). [PubMed: 25402007]
44. R: A Language and Environment for Statistical Computing (R Foundation for Statistical Computing, Vienna, Austria, 2023).
45. pheatmap: Pretty Heatmaps (2019).

46. Katoh K & Standley DM MAFFT multiple sequence alignment software version 7: improvements in performance and usability. Molecular biology and evolution 30, 772–780, doi:10.1093/molbev/mst010 (2013). [PubMed: 23329690]
47. Capella-Gutiérrez S, Silla-Martínez JM & Gabaldón T trimAl: a tool for automated alignment trimming in large-scale phylogenetic analyses. Bioinformatics (Oxford, England) 25, 1972–1973, doi:10.1093/bioinformatics/btp348 (2009). [PubMed: 19505945]
48. Tamura K, Stecher G & Kumar S MEGA11: Molecular Evolutionary Genetics Analysis Version 11. Molecular biology and evolution 38, 3022–3027, doi:10.1093/molbev/msab120 (2021). [PubMed: 33892491]
49. Martin DP, Murrell B, Golden M, Khoosal A & Muhire B RDP4: Detection and analysis of recombination patterns in virus genomes. Virus evolution 1, vev003, doi:10.1093/ve/vev003 (2015). [PubMed: 27774277]
50. Casal PE et al. Evidence for homologous recombination in Chikungunya Virus. Molecular phylogenetics and evolution 85, 68–75, doi:10.1016/j.ympev.2015.01.016 (2015). [PubMed: 25701772]
51. Nguyen LT, Schmidt HA, von Haeseler A & Minh BQ IQ-TREE: a fast and effective stochastic algorithm for estimating maximum-likelihood phylogenies. Molecular biology and evolution 32, 268–274, doi:10.1093/molbev/msu300 (2015). [PubMed: 25371430]
52. Suchard MA et al. Bayesian phylogenetic and phylodynamic data integration using BEAST 1.10. Virus evolution 4, vey016, doi:10.1093/ve/vey016 (2018). [PubMed: 29942656]
53. Yang Z Maximum likelihood phylogenetic estimation from DNA sequences with variable rates over sites: approximate methods. Journal of molecular evolution 39, 306–314, doi:10.1007/bf00160154 (1994). [PubMed: 7932792]
54. Tavaré S Some Probabilistic and Statistical Problems in the Analysis of DNA Sequences. (1985).
55. Hill V & Baele G Bayesian Estimation of Past Population Dynamics in BEAST 1.10 Using the Skygrid Coalescent Model. Molecular biology and evolution 36, 2620–2628, doi:10.1093/molbev/msz172 (2019). [PubMed: 31364710]

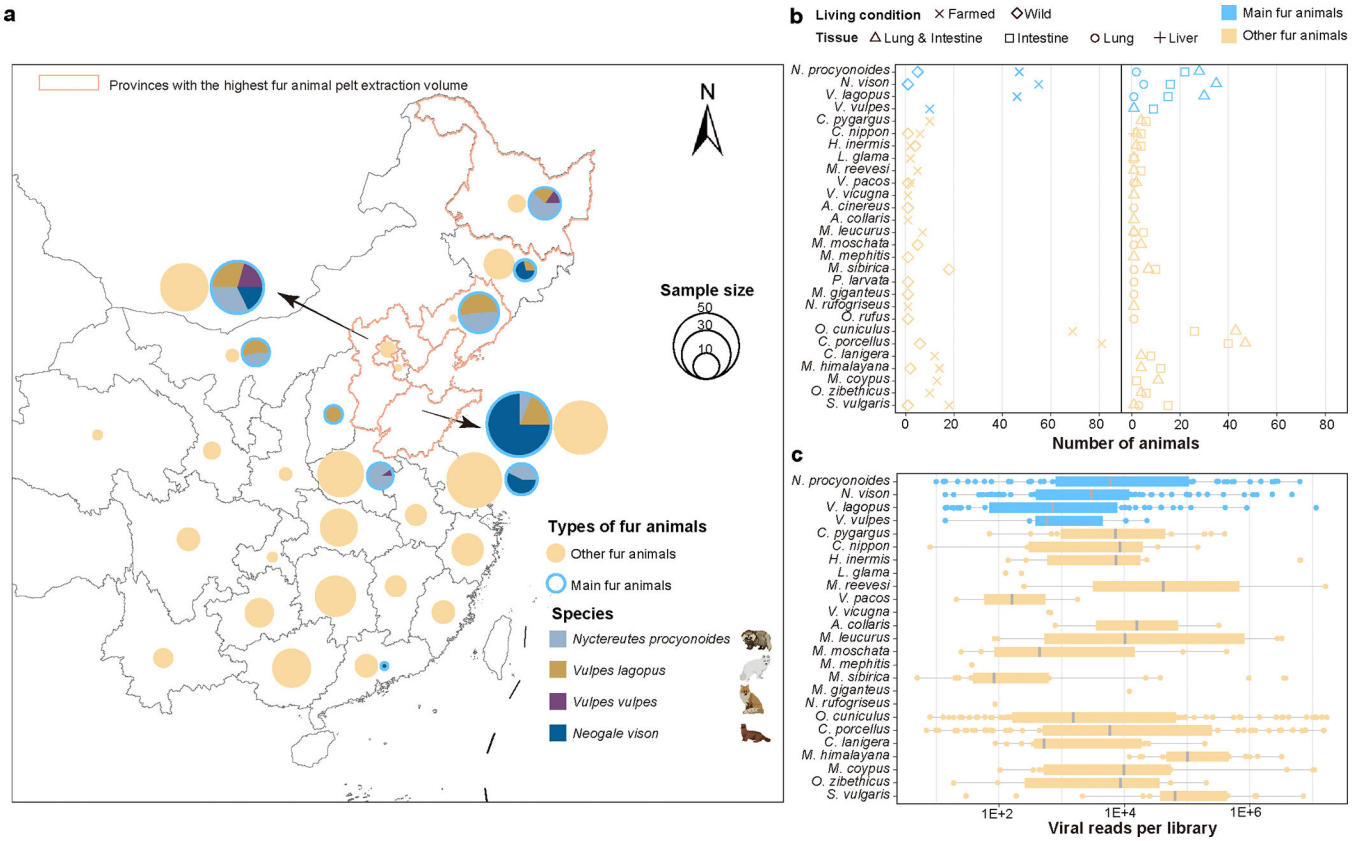

Figure 1. Geographical distribution of animal sampling, fur animal composition, tissue type, library characteristics and viral read counts in this study.

(a) The geographical distribution of 461 deceased animals sampled from multiple Chinese provinces, as well as the main provinces engaged in fur animal husbandry. The fur animals sampled were divided into two categories: (i) the main farmed fur animals that are primarily used for fur production, including mink, foxes, and raccoon dogs; and (ii) the other multipurpose farmed animals, such as rabbits and nutria, that are used for fur production, food consumption, etc. The pie charts show the fur animals sampled. Each main fur animal was assigned a unique colour; the colour of the circle denotes the main or other farmed fur groups. The size of the pie represents the sampling quantity. (b) The distribution of fur animal samples by living condition (left) and sampling organ (right). This study involved dead animals from both captive breeding and wild environments. Sequencing libraries were derived from individual tissues, mostly either the lungs or the intestines, or both the lungs and intestines were used simultaneously. (c) The viral read counts in each library from different species. The box plot shows the median (grey centre line), quartiles (box limits), and the maximum and minimum values (whiskers).

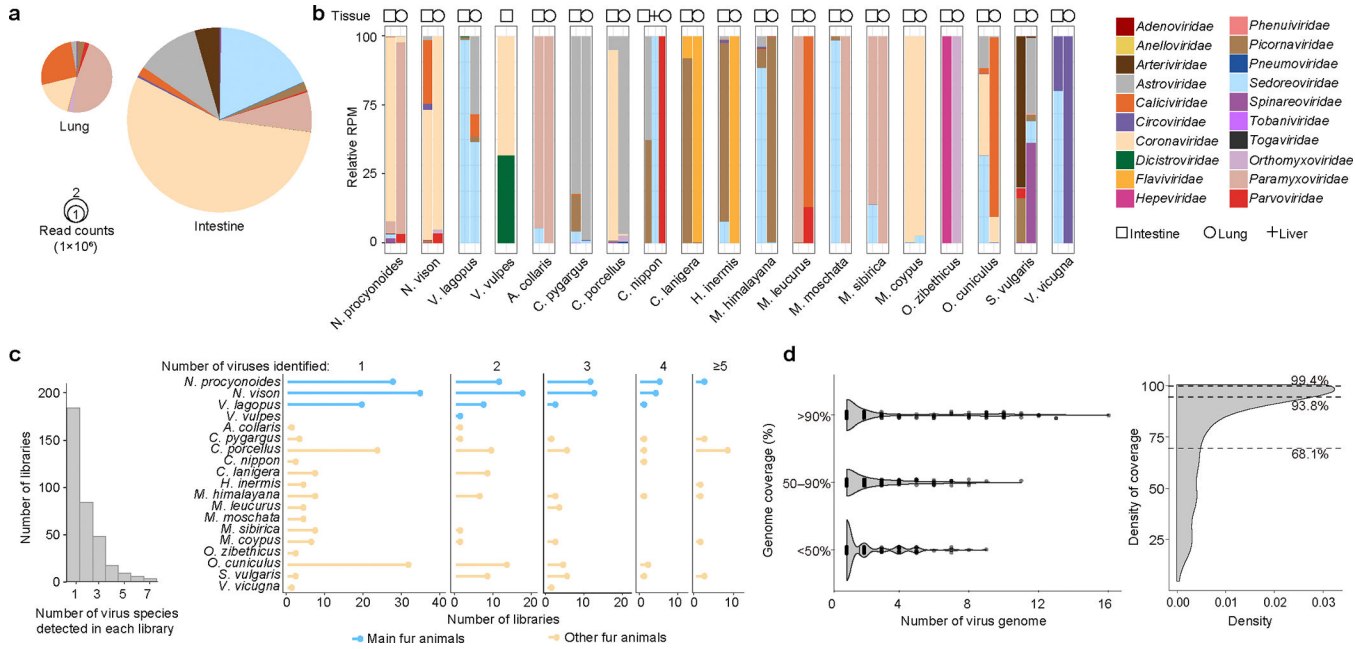

Figure 2. The vertebrate-associated virome of fur animals.

(a) The composition of viruses is displayed at the family level in intestine and lung tissues on the basis of the number of reads with vertebrate-associated viruses. The area of the pie chart represents the total number of virus reads in the intestines or lungs; scale guides of 1 million and 2 million virus reads are shown. (b) The relative abundance of viruses in different tissues of various hosts at the family level. (c) The number of virus species identified in each library. Left, the number of libraries in which 1–7 virus species have been identified. Right, the five boxes list the number of libraries in different animal species in which 1, 2, 3, 4, and ≥5 virus species have been identified. (d) The genome coverage of viral sequences obtained in this study for each sample (left). The violin plot shows the genome coverage of viral sequences for each sample, with the area of each section representing the distribution probability. Right, density plot illustrating the distribution of assembly completeness. The black dashed lines indicate the quartiles and the median.

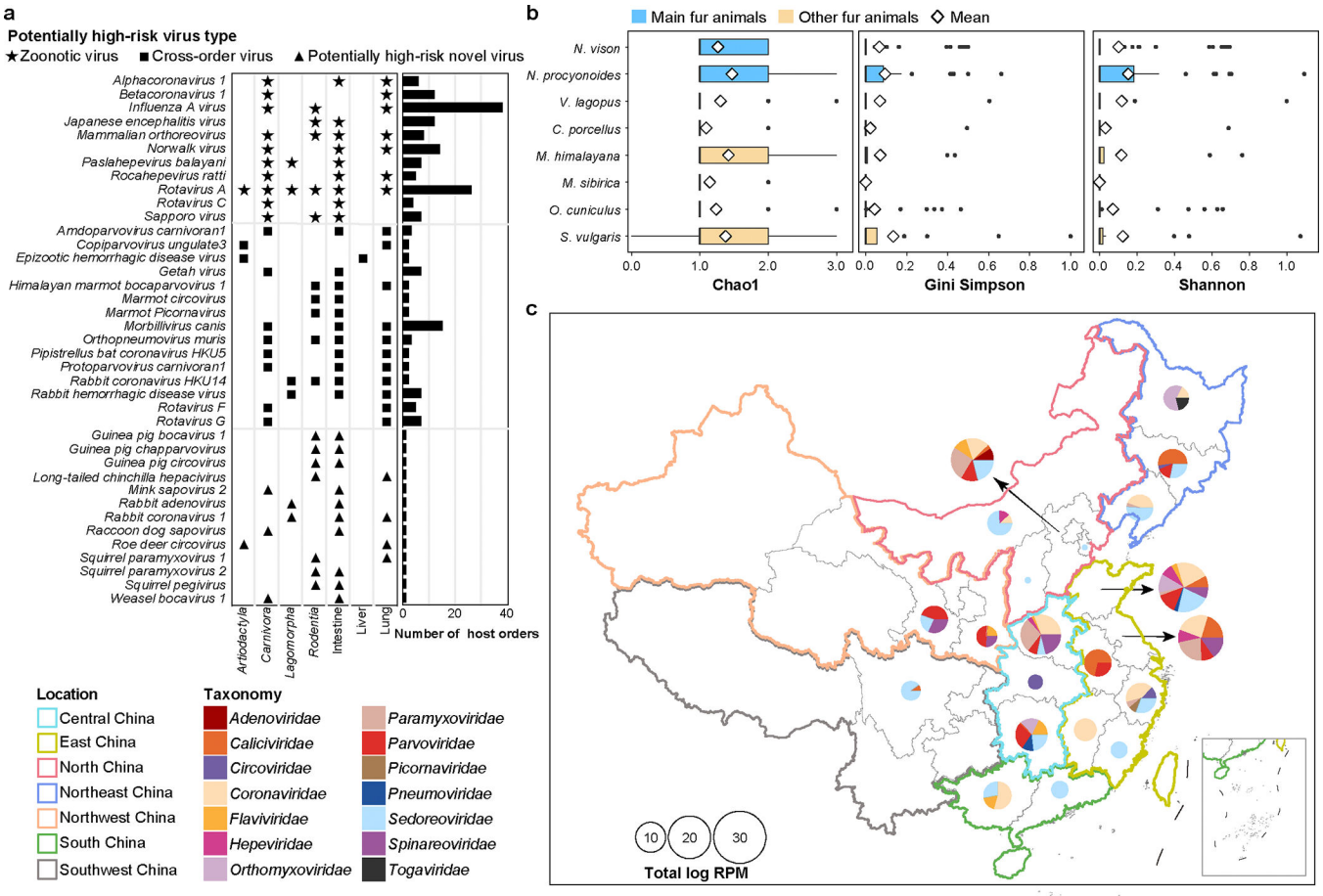

Figure 3. Potentially high-risk virus species and their epidemiological characteristics.

(a) The host range of the potentially high-risk viruses, sourced from NCBI GenBank (right). The stars, squares and triangles represent zoonotic viruses, cross-order viruses and potentially high-risk novel viruses, respectively, denoting identification in this study from the relevant tissue samples, along with the taxonomic order of the identified host. (b) The alpha diversity of potentially high-risk viruses from different species. The Chao1 index was used to determine the variation in viral diversity across diverse animal species, and the Gini-Simpson and Shannon indexes were used to demonstrate the disparities in viral abundance among different animals. The bold black vertical line represents the median, the hollow diamond represents the mean, and the box limits represent the quartiles. The solid black dots indicate values that exceed the lower threshold (25th percentile − 1.5× interquartile range) and upper threshold (75th percentile + 1.5× interquartile range). (c) The distribution of potentially high-risk viruses at the family level detected in various Chinese provinces and the total log-transformed RPM of potentially high-risk viruses belonging to the same family. Total $\log_{10}$ [RPM] represents the sum of the $\log_{10}$ [RPM] of all potentially high-risk viruses within the same province and the same family.